Department of Chemistry

Properties and Applications of $A_2B'B''O_6$ Perovskites: from Fuel Cells to Quasi-Low-Dimensional Magnetism

Sami Vasala

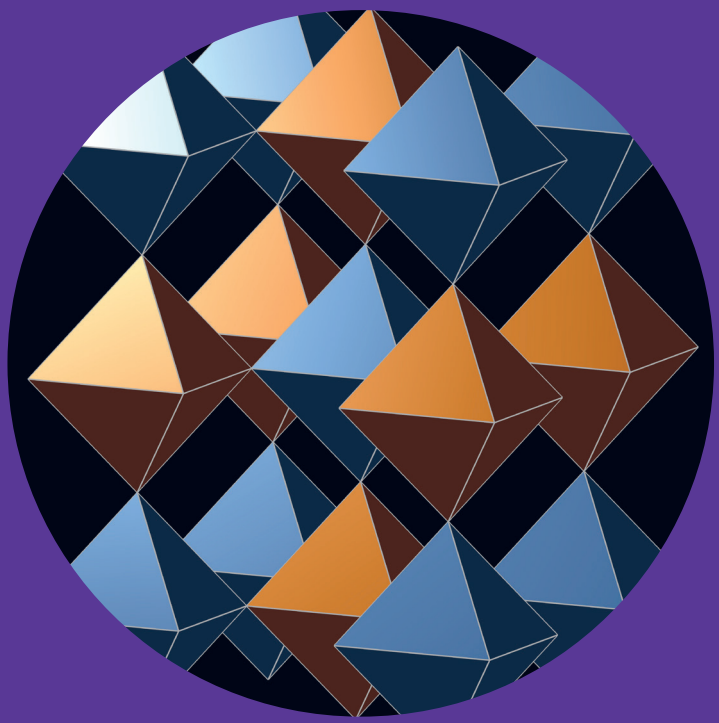

Aalto University

DOCTORAL DISSERTATIONS

Aalto University publication series
DOCTORAL DISSERTATIONS 173/2014

Properties and Applications of $A_2B'B''O_6$ Perovskites: from Fuel Cells to Quasi-Low-Dimensional Magnetism

Sami Vasala

A doctoral dissertation completed for the degree of Doctor of Science (Technology) to be defended, with the permission of the Aalto University School of Chemical Technology, at a public examination held at the lecture hall Ke2 of the school on 21 November 2014 at 12.

Aalto University
School of Chemical Technology
Department of Chemistry
Laboratory of Inorganic Chemistry

Supervising professor
Professor Maarit Karppinen

Preliminary examiners
Professor Bogdan Dabrowski, Northern Illinois University, USA
Associate Professor Christopher Knee, Chalmers University of Technology, Sweden

Opponent
Professor Patrick Woodward, Ohio State University, USA

Aalto University publication series
DOCTORAL DISSERTATIONS 173/2014

© Sami Vasala

ISBN 978-952-60-5936-5 (printed)
ISBN 978-952-60-5937-2 (pdf)
ISSN-L 1799-4934
ISSN 1799-4934 (printed)
ISSN 1799-4942 (pdf)
http://urn.fi/URN:ISBN:978-952-60-5937-2

Unigrafia Oy
Helsinki 2014

Finland

441 697
Printed matter

Aalto University

Abstract

Aalto University, P.O. Box 11000, FI-00076 Aalto www.aalto.fi

Author
Sami Vasala

Name of the doctoral dissertation
Properties and Applications of A2B′B″O6 Perovskites: from Fuel Cells to Quasi-Low-Dimensional Magnetism

Publisher School of Chemical Technology

Unit Department of Chemistry

Series Aalto University publication series DOCTORAL DISSERTATIONS 173/2014

Field of research Inorganic Chemistry

Manuscript submitted 11 August 2014 **Date of the defence** 21 November 2014

Permission to publish granted (date) 28 October 2014 **Language** English

☐ **Monograph** ☒ **Article dissertation (summary + original articles)**

Abstract

Perovskite oxides ABO_3 exhibit a wide range of properties which are of interest both in basic research and in applications. This is largely due to the possibility to incorporate almost any element of the periodic table into the perovskite structure. Partial substitution of elements is also possible, and can lead to chemical ordering of the elements: in case of *B*-site cation substitution, a so-called *B*-site ordered double perovskite $A_2B'B''O_6$ may form. Such double perovskites offer novel properties and applications due the cation order-disorder phenomenon and the combination of two different *B*-site cations. The aim of the present thesis was to gain a greater understanding of the structure, redox behavior and electronic and magnetic properties of $A_2B'B''O_6$ double-perovskite oxides, and the chemical and physical principles behind them.

Among the possible applications for double perovskites, compounds of the type $Sr_2B'MoO_6$ have been considered as anode materials for solid-oxide fuel cells. In this work, $Sr_2B'MoO_6$ perovskites with B' = Mg, Mn, Fe, Co or Ni were examined. Of these, Sr_2MgMoO_6 was found to be redox stable, whereas the compounds with a transition metal at the B' site were not. However, partial substitution of Mg in Sr_2MgMoO_6 by a transition metal could provide materials with improved performance and good redox stability. Partial substitution of Mo in Sr_2MgMoO_6 by Nb or W was also studied. In both cases the compounds remained redox stable, but their electrical conductivities were impaired by the substitution. In case of the Nb-for-Mo substitution, strong correlations between oxygen-vacancy concentration and *B*-site cation ordering was found. Finally, a concept of using an all-ceramic composite material consisting of Sr_2MgMoO_6 and $SrMoO_4$ as an SOFC anode was presented.

The $A_2B'B''O_6$ perovskites also exhibit various magnetic properties, which are of interest in basic research. Compounds with the composition $A_2CuB''O_6$ are especially intriguing, as they may show low-dimensional and/or frustrated magnetic behavior depending on their composition. It is thus useful to examine this group of compounds as a whole, as they can provide information on magnetic properties in solids in general. In the present work two new compounds of this family, Sr_2CuMoO_6 and Sr_2CuIrO_6, were synthesized using a high-pressure synthesis method. In addition, magnetic ground state properties of the quasi-low-dimensional Sr_2CuWO_6 and Sr_2CuMoO_6 were determined. The $Sr_2CuB''O_6$ family of compounds were found to exhibit a transition from quasi-low-dimensional to a more typical antiferromagnetic behavior with increasing *d*-orbital occupancy of the B'' cation. Similar transition was noted in a series of $Ba_2Cu(W_{1-x}U_x)O_6$ compounds with increasing x, with the distinction that both W and U are diamagnetic.

Keywords Double perovskite, Solid-oxide fuel-cell, magnetism

ISBN (printed) 978-952-60-5936-5 **ISBN (pdf)** 978-952-60-5937-2

ISSN-L 1799-4934 **ISSN (printed)** 1799-4934 **ISSN (pdf)** 1799-4942

Location of publisher Helsinki **Location of printing** Helsinki **Year** 2014

Pages 192 **urn** http://urn.fi/URN:ISBN:978-952-60-5937-2

Aalto-yliopisto

Tiivistelmä

Aalto-yliopisto, PL 11000, 00076 Aalto www.aalto.fi

Tekijä
Sami Vasala

Väitöskirjan nimi
A2B′B″O6-tyyppisten perovskiittien ominaisuudet ja käyttökohteet: polttokennoista kvasimatalaulotteiseen magnetismiin

Julkaisija Kemian tekniikan korkeakoulu

Yksikkö Kemian laitos

Sarja Aalto University publication series DOCTORAL DISSERTATIONS 173/2014

Tutkimusala Epäorgaaninen kemia

Käsikirjoituksen pvm 11.08.2014 **Väitöspäivä** 21.11.2014

Julkaisuluvan myöntämispäivä 28.10.2014 **Kieli** Englanti

☐ **Monografia** ☒ **Yhdistelmäväitöskirja (yhteenveto-osa + erillisartikkelit)**

Tiivistelmä

Perovskiittioksideilla ABO_3 tavataan moninaisia ominaisuuksia, jotka ovat kiinnostavia niin perustutkimuksessa kuin sovelluksissakin. Tämä johtuu paljolti siitä, että perovskiittirakenteeseen on mahdollista sisällyttää melkein mikä tahansa alkuaineista. Ionien osittainen korvaus on myös mahdollista, ja tämä voi johtaa ionien järjestäytymiseen: *B*-kationia korvatessa voi muodostua niin kutsuttu *B*-paikan suhteen järjestäytynyt kaksoisperovskiitti, $A_2B'B''O_6$. Nämä kaksoisperovskiitit tarjoavat uusia ominaisuuksia ja sovelluksia johtuen kationien järjestäytymiskäyttäytymisestä ja kahden *B*-kationin yhdistelmästä. Tämän työn tarkoituksena oli tutkia tällaisten $A_2B'B''O_6$ kaksoisperovskiittioksidien rakennetta, hapetus-pelkistyskäyttäytymistä ja sähköisiä ja magneettisia ominaisuuksia, sekä näiden taustalla vaikuttavia kemiallisia ja fysikaalisia ilmiöitä.

Sovelluspuolella $Sr_2B'MoO_6$-tyyppisiä kaksoisperovskiitteja on kaavailtu anodimateriaaleiksi kiinteäoksidipolttokennoihin. Tässä työssä tutkittiin $Sr_2B'MoO_6$-perovskiitteja, missä B' = Mg, Mn, Fe, Co tai Ni. Näistä Sr_2MgMoO_6 oli stabiili sekä hapettavissa että pelkistävissä olosuhteissa, mutta siirtymämetalleja sisältävät yhdisteet eivät olleet. Osittainen Mg:n korvaus siirtymämetallilla saattaa kuitenkin johtaa parempaan suorituskykyyn ja riittävään stabiilisuuteen. Työssä tutkittiin myös Mo:n osittaista korvaamista Nb:lla tai W:lla. Molemmissa tapauksissa yhdisteet olivat stabiileja, mutta korvaus heikensi niiden sähkönjohtokykyä. Korvattaessa Mo:a Nb:lla havaittiin selvä yhteys happivakanssien määrän ja *B*-paikan ionien järjestäytymisen välillä. Lisäksi työssä tutkittiin mahdollisuutta käyttää täysin keraamista Sr_2MgMoO_6-$SrMoO_4$ komposiittia polttokennon anodina.

$A_2B'B''O_6$-kaksoisperovskiiteilla on myös laaja kirjo magneettisia ominaisuuksia, jotka ovat hyödyllisiä perustutkimuksen kannalta. Erityisesti $A_2CuB''O_6$-tyyppiset yhdisteet ovat mielenkiintoisia, sillä niillä on koostumuksesta riippuen havaittu matalaulotteisia ja/tai turhautuneita magneettisia ominaisuuksia. Onkin tärkeää tutkia näitä yhdisteitä kokonaisuutena, sillä ne kertovat materiaalien magneettisista ominaisuuksista yleisesti. Tässä työssä syntetisoitiin kaksi uutta tähän ryhmään kuuluvaa yhdistettä, Sr_2CuMoO_6 ja Sr_2CuIrO_6, käyttäen korkeapainesynteesimenetelmää. Lisäksi työssä tutkittiin Sr_2CuWO_6:n ja Sr_2CuMoO_6:n magneettisten perustilojen ominaisuuksia. Työssä havaittiin $Sr_2CuB''O_6$-yhdisteiden ominaisuuksien muuttuvan kvasikaksiulotteisista tyypillisemmiksi antiferromagneettisiksi B''-ionin *d*-orbitaalien miehityksen kasvaessa. Tällainen muutos havaittiin myös $Ba_2Cu(W_{1-x}U_x)O_6$ yhdisteillä kun x kasvoi, vaikka sekä W että U ovat diamagneettisia.

Avainsanat Kaksoisperovskiitti, kiinteäoksidipolttokenno, magnetismi

ISBN (painettu) 978-952-60-5936-5 **ISBN (pdf)** 978-952-60-5937-2

ISSN-L 1799-4934 **ISSN (painettu)** 1799-4934 **ISSN (pdf)** 1799-4942

Julkaisupaikka Helsinki **Painopaikka** Helsinki **Vuosi** 2014

Sivumäärä 192 **urn** http://urn.fi/URN:ISBN:978-952-60-5937-2

Preface

The work presented in this dissertation was carried out in the Laboratory of Inorganic Chemistry at Aalto University School of Chemical Technology and in the Texas Materials Institute at University of Texas at Austin between June 2009 and September 2014. Academy of Finland, Finnish Funding Agency for Technology and Innovation, Jenny and Antti Wihuri Foundation and Finnish Foundation for Technology Promotion are gratefully acknowledged for financial support.

First and foremost, I wish to thank my supervisor and instructor Professor Maarit Karppinen for all her work in helping me through my doctoral studies. She has always given me a surprising amount of freedom to do my research, yet offered advice and support whenever they were needed. I would also like to thank Professor Hisao Yamauchi for his advices, and Professor John B. Goodenough for letting me visit his group at University of Texas and for sharing his great insight in solid-state physics.

Furthermore, I would like to thank all the people who have collaborated in my work and helped me along the way. Special mentions go to Professor Noriaki Hamada for letting me visit his group at Tokyo University of Science and for his advice on electronic structure calculations; Professor Elvezio Morenzoni and Dr. Hassan Saadaoui for their help with the μSR measurements and analyzes; Professor Omar Chmaissem and Dr. Maxim Avdeev for the neutron diffraction work and their insight and advices considering the magnetic properties of materials; Dr. Jinguang Cheng for his help with high-pressure synthesis; and the whole group of people from National Synchrotron Radiation Research Center, National Taiwan University and National Chiao Tung University, all in Taiwan, for the x-ray absorption measurements.

Great thanks go to all the members of the Laboratory of Inorganic Chemistry, who have made the place a nice environment to work in. I especially wish to thank Dr. Lassi Karvonen, who was my supervisor during my summer work and gave me a good introduction to research work; Dr. Matti Lehtimäki, who was my instructor during my master's thesis work and many the following years, always ready to help when I had a question; Dr. Markus Valkeapää for all the help related to x-ray measurements; Dr. Eeva-Leena Rautama with her tireless assistance with Rietveld refinement and magnetic measurements; and Dr. Jari Malm for his instructions considering atomic layer deposition.

Finally, I wish to thank my family for all their support during these years.

Espoo, October 2014

Sami Vasala

Contents

List of Publications

This doctoral dissertation is mainly based on the following publications which are referred to in the text by their Roman numerals

I S. Vasala and M. Karppinen, $A_2B'B''O_6$ perovskites: a review, *Progress in Solid State Chemistry* (2014), article in press.
DOI: 10.1016/j.progsolidstchem.2014.08.001.

II S. Vasala, M. Lehtimäki, Y. H. Huang, H. Yamauchi, J. B. Goodenough and M. Karppinen, Degree of order and redox balance in *B*-site ordered double-perovskite oxides, $Sr_2MMoO_{6-\delta}$ (*M* = Mg, Mn, Fe, Co, Ni, Zn), *Journal of Solid State Chemistry* **183** (2010) 1007-1012.

III S. Vasala, M. Lehtimäki, S. C. Haw, J. M. Chen, R. S. Liu, H. Yamauchi and M. Karppinen, Isovalent and aliovalent substitution effects on redox chemistry of $Sr_2MgMoO_{6-\delta}$ SOFC-anode material, *Solid State Ionics* **181** (2010) 754-759.

IV S. Vasala, H. Yamauchi and M. Karppinen, Role of $SrMoO_4$ in Sr_2MgMoO_6 synthesis, *Journal of Solid State Chemistry* **184** (2011) 1312-1217.

V S. Vasala, J.-G. Cheng, H. Yamauchi, J. B. Goodenough and M. Karppinen, Synthesis and characterization of $Sr_2Cu(W_{1-x}Mo_x)O_6$: a quasi-two-dimensional magnetic system, *Chemistry of Materials* **24** (2012) 2764-2774.

VI S. Vasala, H. Saadaoui, E. Morenzoni, O. Chmaissem, T.-S. Chan, J.-M. Chen, Y.-Y. Hsu, H. Yamauchi and M. Karppinen, Characterization of magnetic properties of Sr_2CuWO_6 and Sr_2CuMoO_6, *Physical Review B* **89** (2014) 134419-1 - 9.

VII S. Vasala, M. Avdeev, S. Danilkin, O. Chmaissem and M. Karppinen, Magnetic structure of Sr_2CuWO_6, *Journal of Physics: Condensed Matter* (2014), article in press.

VIII S. Vasala, H. Yamauchi and M. Karppinen, Synthesis, crystal structure and magnetic properties of a new double perovskite Sr_2CuIrO_6, *Journal of Solid State Chemistry* **220** (2014) 28-31.

Author's Contribution

Publication I The author performed the literature survey. The author had a major role in writing the manuscript.

Publication II The author defined the research plan together with the co-authors and did the experimental work. The results were interpreted together with the co-authors. The author had a major role in writing the manuscript.

Publication III The author defined the research plan together with the co-authors and did the experimental work except for the XAS measurements. The results were interpreted together with the co-authors. The author had a major role in writing the manuscript.

Publication IV The author defined the research plan, did the experimental work and interpreted the results. The author had a major role in writing the manuscript.

Publication V The author defined the research and did the experimental work. The results were interpreted together with the co-authors. The author had a major role in writing the manuscript.

Publication VI The author defined the research plan together with the co-authors and did the experimental work except for the NPD and XAS measurements, and the μSR measurements and spectral fittings. The results were interpreted together with the co-authors. The author had a major role in writing the manuscript.

Publication VII The author defined the research plan together with the co-authors and synthesized the sample. The results were interpreted together with the co-authors. The author had a major role in writing the manuscript.

Publication VIII The author defined the research plan, did the experimental work and interpreted the results. The author had a major role in writing the manuscript.

List of Abbreviations and Symbols

AFM	Antiferromagnetic
DFT	Density functional theory
DOS	Density of states
HP	High pressure
μSR	Muon spin rotation/relaxation
NN	Nearest neighbor
NNN	Next-nearest neighbor
NPD	Neutron powder diffraction
SOFC	Solid-oxide fuel-cell
TG	Thermogravimetry
XAS	X-ray absorption spectroscopy

A	Atomic site/large cation
B	Atomic site/small cation
B’	Atomic site/small cation with a low oxidation state
B”	Atomic site/small cation with a high oxidation state
g_B	Crystallographic occupancy of cation B
J_i	Magnetic exchange constant for interaction i
N	Number of electrons
S	Bragg-Williams order parameter
T_N	Néel temperature
U	Hubbard on-site coulombic repulsion potential
X	Atomic site/anion

1. Introduction

The development of humankind from hunter-gatherers to modern societies has largely depended on the use of technology. This progress has been made possible by the development of materials; from bronze and iron of the ancient times to silicon of the modern era, new materials with improved or novel properties have often been the key to technological advances. This formula of advancement through development of new materials holds for the foreseeable future: building the world of tomorrow requires new materials for applications in fields such as electricity generation and storage, transportation, electronics and information technology, and health care.

Of the many types of materials known, those crystallizing in the perovskite structure are among the most intensely studied.[1] The perovskite structure ABX_3, shown in Figure 1, appears deceitfully simple: in the ideal cubic case the structure consists of a large cation at the *A* site, a smaller cation at the octahedrally coordinated *B* site, and bonding with both cations an anion *X*, which most often is oxygen. The $BX_{6/2}$ octahedra form a corner-shared network in all three crystallographic directions, with the remaining cuboctahedral voids filled by the *A* cation.[2]

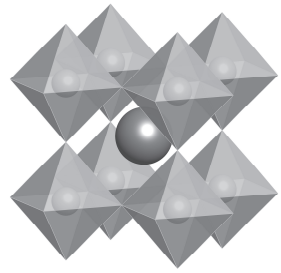

Figure 1. Schematic of the perovskite structure ABX_3. Cation *A* is shown as the large sphere at the center, whereas cation *B* is presented by the smaller spheres inside the octahedra. Anions *X* reside at the vertices of the octahedra.

Despite this apparent simplicity, perovskite compounds have several fundamentally interesting chemical and physical properties.[1,3] They may be insulators with a wide range of band-gap values, metals, half-metals[4,5] or even superconductors.[6] They exhibit magnetic orderings ranging from antiferromagnetic to ferri- and ferromagnetic,[7,8] but can also show magnetic frustration with no apparent long-range spin order.[9,10] Perovskites may also show high ionic conductivities[11,12] and good catalytic properties.[13] What is more, they may have many of these properties simultaneously, resulting in combined properties, as

in multiferroic compounds.[14,15] As a result, perovskite materials are of great technological interest, with a range of possible applications such as dielectrics or magnetic memory components in electronics,[5,16,17] electrode and electrolyte materials for fuel cells,[11,18,19] photocatalysts for water splitting,[20] and as recently discovered, components for solar cells,[21] to name just a few.

The wide range of properties in perovskites stems largely from their exceptional structural and compositional flexibility.[2,22] The $BX_{6/2}$ octahedra can expand, contract or tilt in order to compensate for non-ideal ionic size ratios of the different cations, and in case of electronic instabilities, the octahedra can distort or the cations may shift from their ideal positions. What is especially important is that it is often possible to make partial substitutions or to create vacancies at any of the three sites of the structure. As a result of this flexibility, the perovskite structure can accommodate almost all of the elements of the periodic table, in one form or another.

1.1 Double Perovskites

The compositional flexibility of the perovskite structure is especially notable in the case of cation substitution. Both the *A* and *B* cations can be partially substituted with either iso- or aliovalent cations, resulting in a large number of possible mixed compositions. What is more, chemical ordering of the substituted cations is possible, and can happen either at the *A* or *B* site, or in both simultaneously. Ordering of the *A*-site cations is somewhat rare, whereas ordering of the *B*-site cations is quite common, especially when the site is occupied by two cations in equal amounts (1:1 substitution).[2,23,24]

In the ordered 1:1 *B*-site substituted case with two cations, *B*' and *B*", a so-called *B*-site ordered double-perovskite $A_2B'B''X_6$ is formed. The cations *B*' and *B*" can order in three different ways, as presented in Figure 2.[23,25] In by far the most common case the cations alternate in all three crystallographic dimensions (Figure 2(a)), creating a rock-salt-type arrangement, also known as the elpasolite structure, after the mineral K_2NaAlF_6. The *B*-site cations may also form a layered order, where the cations alternate only in one direction, as presented in Figure 2(b). This ordering is stabilized only in rare cases where one of the *B*-site cations is a Jahn-Teller (JT) active ion and the difference in *B*-site cation radii is suitable. A columnar order of the *B*-site cations is also possible, with cations alternating in two directions, as shown in Figure 2(c). However, this ordering has only been found in a few $A'A''Mn_2O_6$ compounds where the *A* site is occupied by two different cations, and there is charge disproportionation of Mn and a JT distortion of the resulting Mn^{III}.

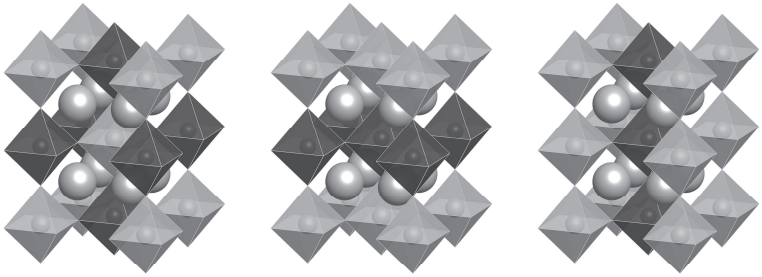

Figure 2. Schematic of the three *B*-site cation arrangements in $A_2B'B''X_6$ perovskites. (a) Rock-salt, (b) layered and (c) columnar order.

The *B*-site cation ordering in the $A_2B'B''X_6$ perovskites may not be complete. The degree of cation order can be quantified using the Bragg-Williams long-range order parameter[26]

$$S = g_B - 1,$$

where g_B is the occupancy of one of the *B*-site cations at its correct site. The degree of order may take any value from $S = 0$ (completely disordered) to $S = 1$ (completely ordered), and depends mainly on charge difference between the two *B*-site cations: typically, when the charge difference is smaller than two the compounds are disordered and when it is larger than two the compounds are ordered. This is due to an increase in electrostatic repulsion between the more highly charged *B*" cations as the cation charge difference increases. Size difference between the two *B*-site cations is another common cause for ordering, especially when charge difference is two or less. Generally, the larger the size difference, the more probable cation ordering is, due to increase in lattice strain.[23,25,27]

The possibility of cation ordering adds to the complexity and modifiability of the perovskite compounds. Such order-disorder phenomena are of fundamental interest by themselves, but the ordering also affects many of the physical properties of these compounds. This is perhaps most notably exemplified in the case of Sr_2FeMoO_6, which in an ordered state is a ferrimagnetic half-metal, with notable tunneling magnetoresistance even at room temperature. However, the half-metallic and magnetoresistive properties are strongly affected by the *B*-site cation order, and disordered compounds lose both of these properties.[28,29]

In perovskite compounds the *B*-site cations typically govern many of the fundamentally and technologically interesting properties, such as electrical conductivity and magnetic order. Having two different *B*-site cations in a perovskite structure allows for various novel combinations of different elements, ranging from 3*d*, 4*d* or 5*d* transition metals through lanthanides or actinides to main group elements, many of them in various different oxidation states. This possibility of combining different kinds of elements together with various

degrees of cation ordering can result in a wide range of intriguing properties in the $A_2B'B''X_6$-type perovskites, which were the main focus of this work.

1.2 Scope of the Present Thesis

The overarching objective of the present work was to understand the various properties of the $A_2B'B''X_6$ perovskite system, and moreover, the physical principles behind them. As stated before, the anion X in perovskites is most often oxygen, and in this work only oxide compounds were considered. A broad overall view at these compounds was taken in the form of a literature survey; *ca*. one thousand $A_2B'B''O_6$-type compounds, both ordered and disordered, were reviewed.[I] These compounds show a rich variety of structural, electronic and magnetic properties, which were discussed together with their possible applications. In addition to this broad overview, two more specific subjects were studied more in depth: the application of $Sr_2B'MoO_6$-type compounds as solid-oxide fuel-cell (SOFC) anodes, and the intriguing quasi-low-dimensional and frustrated magnetism found in $A_2CuB''O_6$-type compounds.

Sr_2MgMoO_6 has been found to be a promising compound as an anode material for SOFCs, and several other similar $Sr_2B'MoO_6$ perovskites with B' = Mn, Fe, Co or Ni have also been considered from this point of view. [19,30–34] As a part of this work, their applicability as anode materials was examined.[II] In addition, substituting the electrocatalytically active Mo of Sr_2MgMoO_6 by neighboring elements Nb or W was studied, as this had not been done before.[III] The stability, reducibility and electrical conductivity of these compounds were considered. Finally, effects of a common impurity phase $SrMoO_4$ to the properties of Sr_2MgMoO_6 was investigated, together with a possibility of using an all-ceramic composite material consisting of Sr_2MgMoO_6 and $SrMoO_4$ as an SOFC anode.[IV]

Compounds with the composition $A_2CuB''O_6$, where A is Sr or Ba and B'' is a hexavalent ion, may exhibit low-dimensional and/or frustrated magnetic properties depending on their composition.[35–44] This relatively small group of compounds forms a simple model system with interesting variability in properties, which have not yet been thoroughly studied. It is thus of interest to examine this group as a whole, as they can provide information on magnetic properties in solids in general. In the present work two new compounds of this family, Sr_2CuMoO_6 and Sr_2CuIrO_6, were synthesized.[V,VIII] In addition, magnetic ground state properties of Sr_2CuWO_6 and Sr_2CuMoO_6 were determined[VI,VII] and the magnetic properties of this whole family of compounds were compared.

2. Experimental Methods

In the course of this work several $A_2B'B''O_6$-type double perovskite compounds were synthesized and characterized, some of them new, some already known. While most of the samples were synthesized at ambient pressure using either standard solid-state synthesis or a sol-gel process, high-pressure synthesis was also employed when necessary, as described in Chapter 2.1.

The samples were characterized using a range of standard analysis methods used in the fields of solid-state chemistry and physics. X-ray powder diffraction together with Rietveld refinement was used to examine crystal structures both at room temperature and at high temperatures. Reducibility and redox stability were studied with thermogravimetric (TG) analysis, and oxygen content was determined by coulometric titration. Electrical conductivities of samples were measured in a four-probe setup, and in case of semiconducting samples, diffuse-reflectance spectroscopy in the UV-Vis-IR range was used to determine optical band-gaps. Magnetic properties either as a function of temperature or external magnetic field were measured using a superconducting quantum interference device magnetometer.

In addition to these methods, a few somewhat more infrequent methods were used in this work to analyze the materials. These included x-ray absorption spectroscopy (XAS), muon spin relaxation/rotation (μSR), neutron powder diffraction (NPD) and electronic structure calculations, and these methods are briefly discussed in Chapters 2.2-2.5, respectively.

2.1 High-Pressure Synthesis

Nearly one thousand $A_2B'B''O_6$-type perovskite compounds have been reported in the literature, most of them synthesized under ambient pressure.[I] However, about 50 of these compounds have been realized through high-pressure (HP) synthesis. HP synthesis can often be used to stabilize metastable high-pressure phases at ambient temperature by quenching samples from high temperatures while keeping them under pressure. The high pressure prefers structures with smaller unit-cell volumes, and as the perovskite is a relatively densely packed structure, it is often formed during HP synthesis.[45]

In the present work Sr_2CuMoO_6 was synthesized using high pressure.[V] Attempts to synthesize this compound in ambient pressure resulted in a mixture of $SrCuO_2$ and $SrMoO_4$, both of which have the transition metals in four-coordination. It was thus presumed that the perovskite structure with the transition metals in a higher six-coordination could form under pressure. This was indeed the case, and the compound was synthesized using a cubic-anvil apparatus at a pressure of ~4 GPa and a temperature of ~900 °C.

It is also possible to stabilize elements in uncommonly high oxidation-states using high oxygen-pressure during synthesis. For example, many $A_2B'IrO_6$

perovskite compounds with hexavalent iridium have been stabilized using this method.[46–51] Some of these compounds form even at ambient pressures under oxygen atmosphere, but are notably oxygen deficient due to a reluctance of the Ir to oxidize to Ir^{VI} at these conditions.[46] However, HP synthesis combined with an appropriate oxygen source can be used to uphold very high oxygen-pressures, oxidizing Ir to Ir^{VI} or close.

In this work Sr_2CuIrO_6 was synthesized with the aid of high oxygen-pressure.[VIII] The compound did not form at ambient pressure even as an oxygen deficient phase, but required the use of high pressure. The synthesis conditions were similar to those of Sr_2CuMoO_6, but $KClO_3$ was added to the starting material mixture to serve as an oxygen source, as it decomposes at high temperatures, releasing oxygen.[52]

2.2 X-ray Absorption Spectroscopy

X-ray absorption spectroscopy is a very strong element-specific method for examining oxidation states and local coordinations of elements in solid compounds.[53,54] In XAS, a core-electron of an element is excited to an empty state above the Fermi level using x-ray radiation, typically from a synchrotron radiation source. The excitations are limited by the dipole selection rules, which state that ideally only transitions with angular momentum change $\Delta l = \pm 1$ are allowed. In case of transition metal oxides, the most interesting transitions are often either from an oxygen *s* core-level to a *p*-like final state, or from a transition metal *p* core-level to a *d*-like final state. The electron excitations are evident in the absorption spectrum as edge-like jumps when the x-ray energy matches the excitation energy. Naming of these absorption edges is based on the initial shell of the excited electron, so the *K* edge corresponds to an initial $1s$ core states, whereas L_1, L_2 and L_3 edges correspond to $2s$, $2p_{1/2}$ and $2p_{3/2}$ initial states, respectively.

The absorption edge energy can be used to probe the formal oxidation state of an element: the edge shifts to higher energies as the oxidation state of an element is increased. A simple explanation of this behavior is that it becomes more difficult to excite the core-electrons of a more oxidized element as the nucleus is less shielded and has a higher effective charge. Comparing absorption edge energies of an element in an unknown sample to those of known oxidation states can reveal the elements oxidation state.

In addition to the absorption edge energy, the absorption feature intensity may also contain information about the electronic state of an element. For example, the absorption intensities of transition metal $L_{2,3}$ edges in oxide compounds with unoccupied *d*-like final states near the Fermi level have been found to be sensitive to the *d* electron occupancy of the element.[47,50] Also, in compounds with a transition metal in octahedral coordination these $L_{2,3}$ absorption features are often found to be split into two separate peaks due to a crystal field splitting of the transition metal d orbitals, with the two peaks corresponding to t_{2g}- and e_g-derived final states.[47,50,55,56] In case of $3d$ transition metals the separation of these peaks may be weak, but with $4d/5d$ elements

the separation is often more notable due to their stronger crystal field splitting. Furthermore, in many binary oxides the separation of these peaks is somewhat poor due to a formation of a wide conduction band, whereas for the *B*-site cations in ordered double perovskites the t_{2g}- and $_{eg}$-like states are often well separated, as the *B*-site cations are more isolated and form narrower bands. Thus the relative intensities of the absorption features related to excitation to the t_{2g}- and e_g-derived bands can tell about the electron population of these bands.

The aforementioned effects are exemplified in Figure 3, which shows the Mo L_2 x-ray absorption spectra of MoO_2, MoO_3 and Sr_2MgMoO_6 measured at the National Synchrotron Radiation Research Center in Taiwan. Firstly, the absorption edge is shifted to a higher energy when moving from MoO_2 to MoO_3 as the oxidation state of Mo increases from IV to VI. The absorption edge of Sr_2MgMoO_6 roughly matches that of MoO_3, indicative of the same VI formal oxidation state of Mo in both compounds. Also, in Sr_2MgMoO_6 a clear separation of the two absorption features with t_{2g}- and e_g-derived final states is seen, as expected for the relatively isolated Mo ions with a notable crystal field splitting.

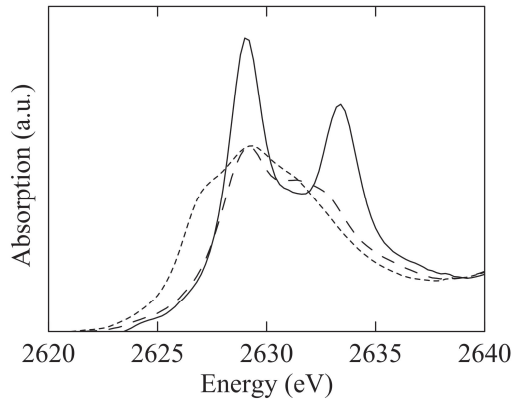

Figure 3. Mo L_2-edge XAS spectra for MoO_2 (short dash), MoO_3 (long dash) and Sr_2MgMoO_6 (solid).

It is thus evident that XAS can essentially probe the empty electron states above the Fermi level. This can be very useful, as it is often possible to compare a measured XAS spectrum to empty densities-of-states (DOS) obtained from electronic structure calculations.[57–60] In the case of metal oxides, the oxygen *K*-edge XAS with 2*p*-like final states is often optimal for such comparison: due to the notable covalent character of these compounds, the O 2*p* orbitals are hybridized with the cations, and the O *K*-edge spectrum contains information about the empty states of all the ions.

An x-ray absorption spectrum is typically comparable to a calculated DOS only in approximation. The calculated DOS represents a ground state band structure of the compound, whereas in XAS the excited electron and the remaining core hole affect the electronic structure of the probed element. The

use of O *K* edge XAS in case of metal oxide compounds is somewhat fortunate, however: the core hole remains on the oxygen 1*s* orbital, whereas the hybridized final states have more weight from the metal elements due to the electronegativity difference between the metals and oxygen. The O 1*s* orbital only weakly affects these final states, and often the O *K* XAS spectra may be compared to calculated oxygen partial DOS even without taking the core-hole effects into account.[54,57–60]

2.3 Muon Spin Relaxation/Rotation

Muon spin relaxation/rotation is a somewhat rarely used yet very sensitive probe towards local magnetic fields in a material. It can detect small fields, causes no disturbance to the system, and has no restrictions on materials to be studied. What is more, unlike many other magnetic measurement methods, μSR works even in zero external magnetic field.[61–63]

The muon is an elementary particle with a spin of ½ and a lifetime of ~2.2 μs. In the μSR experiment, a ~100 % spin polarized muon is planted in the sample under study. The spin of the muon interacts with the local magnetic fields of the sample, resulting in Larmor precession and/or depolarization/relaxation of its initial polarization. The muon eventually decays emitting a positron that can be detected. Importantly, the emission of the positron is asymmetric and happens preferably in the direction of the muon spin. Thus by detecting the asymmetry in the positron emission the time evolution of the muon spin polarization can be determined, and information on the local magnetic fields in the sample can be obtained.[61–63]

The μSR measurements in this work were performed at the Paul Scherrer Institute in Switzerland. Figure 4 shows μSR spectra measured for Sr_2CuWO_6 at three different temperatures as an example. At 30 K only a slow depolarization is seen, typical of paramagnetic behavior. On the other hand, below ~24 K clear oscillations appear in the spectra, indicative of magnetic order with the muons precessing in the local magnetic field. Thus a the magnetic transition temperature can be obtained from the μSR data, and fitting a model to the measured spectra can also reveal the evolution of the internal magnetic field as a function of temperature.

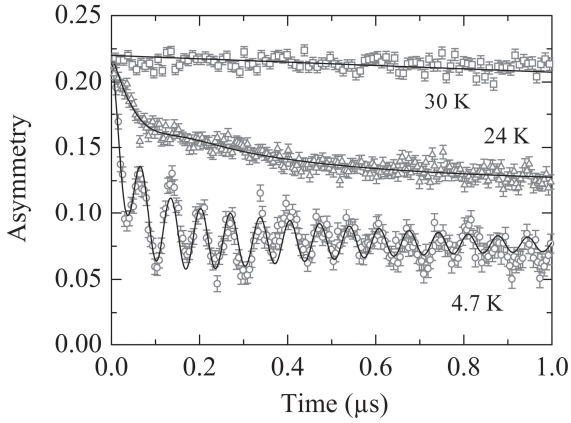

Figure 4. μSR spectra of Sr_2CuWO_6 measured at three different temperatures.[VI]

2.4 Neutron Powder Diffraction

The use of neutron powder diffraction has two big benefits when studying transition metal oxides: it can sensitively detect oxygen and it can be used to determine magnetic structures.[64] As the crystal structure, including oxygen positions, is important for material's properties, and the transition metal oxides are typically magnetic, NPD is often a key method in their study.

In case of the rather more commonly used x-ray diffraction, the x-rays interact primarily with the electron clouds of the elements in the sample. Thus the diffraction intensity depends on the number of electrons of the elements, and detecting elements with small number of electrons, such as oxygen, becomes difficult, especially if there are heavier elements present. Neutrons, on the other hand, interact mostly with the atomic nuclei, and their diffraction depends on the atomic isotopes. The neutron scattering lengths are not linearly dependent on the atomic number, so even light elements can often be detected.

Neutrons also have a spin, which means that they interact with magnetic moments in the sample. Thus they can be used to probe the magnetic structure of a compound, and NPD is often the best method for determining the magnetic ground state of a compound.[64]

In the present work high resolution time-of-flight NPD data measured at the Spallation Neutron Source, Oak Ridge National Laboratory were used to determine the structure of Sr_2CuWO_6 at low temperatures. While this instrument provided great resolution for structural study, it was unable to detect the weak magnetic reflections in this sample. Thus high-flux NPD data collected at Australian Nuclear Science and Technology Organisation in Australia were used to study the magnetic structure of this compound. Figure 5 shows the measurements above and below the magnetic transition temperature as an example. Weak new peaks appear at low temperatures, and the difference of these curves (Figure 5, inset) clearly shows several peaks of magnetic origin.

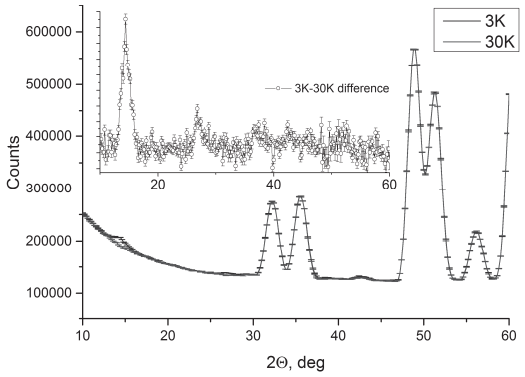

Figure 5. NPD measurement data for Sr_2CuWO_6 at 3 and 30 K. Inset shows the difference curve of the two measurements.[VII]

2.5 Electronic Structure Calculations

Calculating the electronic structure of a material is often of interest, as it can predict or help understand many of the material's properties, such as electrical transport or magnetism. Thanks to the great increase in computing power in the last twenty years, these calculations have become possible even on normal desktop computers, making them available for any researcher.

The premise of quantum mechanics is that the wave function obtained by solving the Schrödinger equation for the system under study essentially describes the whole system and predicts all of its properties. However, in case of a system with N electrons, finding the wave function is hindered by the electron-electron interactions, which would require solving a very complicated many-body problem with $3N$ spatial coordinates. This is not feasible for any large systems, and calculating the electronic structure would be impossible without some great advances in computational methods. These days the methods most commonly used in calculating the ground state electronic structure of solid compounds are based on the density functional theory (DFT), which simplifies the many-body problem into a more manageable problem of non-interacting electrons in an effective potential.[65]

This simplification if based on two theorems by Hohenberg and Kohn,[66] which state that 1) for a given system the ground-state energy of the Schrödinger equation is a unique functional of the electron density, and 2) the density that minimizes the energy of this functional is the true equilibrium electron density. The first statement means that the electron density uniquely determines the ground state of the system and its properties. Thus in the calculations only three spatial coordinates of the electron density need to be considered, instead of $3N$ of all the electrons. The second statement means that even though the energy functional needed in the calculations is not known, it can in principle be found by varying the electron density until the energy is minimized. Furthermore, Kohn and Sham[67] showed that it is possible to find the right electron density by solving equations involving only single electrons in an effective potential. However, the effective potential depends on the electron

density, which leads to a self-consistent iterative process of finding the ground state, where the effective potential is calculated based on some initial electron density, and a new electron density is calculated using this potential. This process is then continued until the initial and resulting electron densities are considered equal.

The major problem in DFT is that exact functionals for electron exchange and correlation are not known. These functionals can be rather well approximated, most commonly either by the local-density approximation, which uses a known functional of a uniform electron gas applied at a local position, or by various generalized-gradient approximations, which take into account the gradient of the electron density as well. While hugely successful, these exchange-correlation functionals often fail to describe systems with strong electron-electron correlations, such as transition metal oxides. These correlations can be taken into account for example by using the Hubbard U parameter (DFT+U formalism), which models the on-site electronic repulsion.[68] However, the value of U is not known beforehand, and often a range of values is tested in order to divulge the effect of the parameter to the calculated results. On the other hand, it is sometimes possible to compare calculations to experimental results in order to find a suitable value of U, and in this work XAS spectra were used as experimental references when determining U. As stated before, XAS essentially probes the empty electron states above the Fermi level, and can be compared to calculated DOS, especially in case of the O K-edge XAS. Thus comparing DOS calculated with different values of U to measured XAS spectra was able to give an estimate for the value of U.

The objective of the DFT electronic structure calculations in this work was to determine the values of the most relevant magnetic exchange interaction constants (J_i) in Sr_2CuWO_6 and Sr_2CuMoO_6, as knowing the exchange constants would help understand the quasi-low-dimensional magnetic properties of these compounds. One commonly used method for calculating the J_i is the so-called mapping method. Within this method, total energies of several magnetic configurations are calculated, and the energy differences between these magnetic states are used to calculate the J_i using an appropriate spin Hamiltonian.[69–72] In the present work the mapping method was used to calculate the nearest- and next-nearest-neighbor interactions between Cu ions in Sr_2CuWO_6 and Sr_2CuMoO_6, and the results were interpreted in order to explain their magnetic behavior.

3. Solid-Oxide Fuel-Cell Anodes

The solid oxide fuel cell is an electrochemical device that converts the chemical energy of a fuel directly to electrical energy. SOFCs consist of three main components: a cathode (or an air electrode), an anode (or a fuel electrode) and an electrolyte, as shown in Figure 6. At the cathode, O_2 molecules from air are reduced to O^{2-} ions by electrons received from an external circuit. The O^{2-} ions travel through the electrolyte from the cathode to the anode, where they oxidize the fuel. Electrons freed in the oxidation process are transferred to the external circuit, generating an electrical current that can be used to do work.

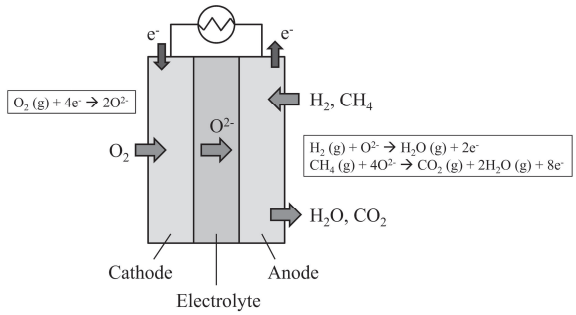

Figure 6. Schematic of a solid oxide fuel cell, together with the overall electrode reactions. Oxidation of H_2 and CH_4 fuels are shown as an example.

The advantage of SOFCs is their high chemical-to-electrical energy conversion efficiency: unlike conventional heat engines, fuel cells are not subject to the Carnot-cycle limitations. As the devices operate at high temperatures, typically in the range of 800-1000 °C, excess heat generated by the cell can also be used in combined heat and power applications, or to run a gas turbine. The most common applications for SOFCs range from large-scale power plants to portable auxiliary power units.[73–77]

There have been several hindrances in the commercialization SOFCs, most notably the high cost of construction and degradation of materials during operation, both caused at least partially by their high operating temperatures. Decreasing the operating temperature below 800 °C would significantly improve the long term stability and allow the usage of cheaper materials in some of the cell components. However, lowering the operating temperature lowers reactivity and cell efficiency, and in order to counteract this more efficient electrolyte and electrode materials are needed.

The second obstacle in the development of SOFCs is related to the use of fuels. Even though in principle SOFCs could utilize any combustible fuel, in practice the current SOFCs with Ni-based anodes can operate only on hydrogen or pre-reformed hydrocarbon fuels. This is due to the fact that Ni catalyzes

formation of graphitic carbon on the anode, which is detrimental to the anode performance.[74,77,78] Direct utilization of hydrocarbon fuels without reforming would be beneficial, but would require new anode materials to be developed for SOFCs. Ceramic materials generally have a better stability than Ni when hydrocarbon fuels are used and they have thus been investigated as alternative anode materials for SOFCs. However, the development of all-ceramic anodes is still in the state of finding suitable candidates, as no material with performance comparable to the traditional Ni-based anodes has yet been found.

The anode of the SOFC facilitates the oxidation of the fuel: thus the anode material has to be electrocatalytically active towards fuel oxidation.[75,78,79] It also has to be electronically conductive in a highly reductive environment. Typical target for the minimum electrical conductivity of the electrode materials is in the order of 100 S/cm, but values as low as 1 S/cm may suffice with well-distributed current collection.[79] Ionic conductivity would also be beneficial, as it would increase the reactive surface area of the anode: in case of a purely electronically conducting anode material, such as the commonly used Ni, the electrochemical reactions occur only at the so called three-phase boundary, a narrow line of contact between the gas phase, the electrolyte and the anode, as shown in Figure 7(a). On the other hand, a mixed ionic and electronic conductivity (MIEC) of the anode material greatly extends the effective electrochemical reaction zone, as in principle the whole electrode surface can function as a reaction site, as presented in Figure 7(b). The ionic conductivity of an oxide material typically takes place by oxide ions moving between vacant oxygen sites, and certain amount of oxygen vacancies would therefore be essential for high ionic conductivity.

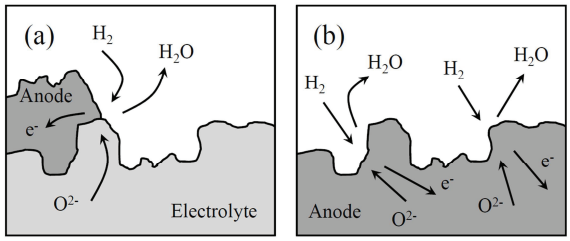

Figure 7. Schematic of (a) a purely electronically conducting anode, where the oxidation reaction takes place only at the three-phase boundary and (b) a mixed ionically and electronically conducting anode, where the oxidation reaction can happen at the whole surface.

Development of a ceramic SOFC anode would thus at the minimum require a material that is electrically conductive and electrocatalytically active below 800 °C, stable under reducing conditions, but still reducible enough to form oxygen vacancies. The easiest place to start in the search for such a material is to find compounds with high electrical conductivities. In case of the $A_2B'B''O_6$ perovskites, most of the compositions are insulators or semiconductors.[1] Semiconducting behavior is often enough for the anode materials, as electrical conductivity of semiconductors increases with increasing temperature and the

SOFC operates at high temperatures. In case of ordered $A_2B'B''O_6$ perovskites, the electronic bandwidth affecting the electrical conductivity depends among other things on the spatial overlap of the ionic orbitals: often highest values of electrical conductivity are found in compounds with $4d/5d$ transition metal elements at the *B*-site due to their extended *d* orbitals, which result in wide conduction bands.[80,I] However, many of these heavier transition metal elements are rare and expensive. Perhaps for this reason the study of double perovskites for SOFC anode applications has been focused on compounds with the more abundant elements Mo or Nb.[19,30–34,81–83] While the Nb-containing compounds often show relatively low electrical conductivities,[I] the $A_2B'MoO_6$-type double perovskites have gained a lot of interest due to possible high electrical conductivities and good catalytic activities.

3.1 Sr_2MgMoO_6

Of the Mo-containing double perovskites, Sr_2MgMoO_6 has been most extensively studied as a SOFC anode.[19,30,84–86] Single fuel-cell tests by Huang *et al.*[19,30] using this material indicated a good performance in both H_2 and CH_4. Additionally, the cell performance under CH_4 was stable without carbon formation and Sr_2MgMoO_6 was even found to tolerate small concentrations of H_2S in fuel. The material has been found to be stable both in oxidizing and reducing conditions, and to be slightly reduced in the anode conditions, allowing for formation of oxygen vacancies. In Sr_2MgMoO_6, the $Mo^{VI/V}$ redox pair is responsible for the electronic conductivity, and the conductivity increases with increasing reduction. Samples synthesized in reducing conditions typically show conductivity values in the order of 1 S/cm at 800 °C under reducing atmosphere, enough for an SOFC anode.

However, Bi and Zhu[87] found a much poorer performance in their fuel cell tests using Sr_2MgMoO_6 as an anode. Instead they noted that the Pt current collector and $(La,Ce)O_{2-d}$ buffer layer used in cell tests had a significant role in the cell performance and that Sr_2MgMoO_6 itself was rather inactive. Similarly, in a study by van den Bossche and McIntosh[88] Sr_2MgMoO_6 showed poor catalytic activity towards CH_4 oxidation, probably due to a poor oxygen release capability. These results are rather contradicting, as Huang *et al.*[19,30] tested their cells without Sr_2MgMoO_6, and found notably reduced performance with cells using only $(La,Ce)O_{2-d}$ and Pt, especially when using CH_4 as a fuel. Similarly, an anode with a Pt mesh buried into Sr_2MgMoO_6 showed 15-25 % lower performance than one with an exposed Pt mesh, but this performance drop was still much smaller than that noted by Bi and Zhu.

These discrepancies may in part be explained by different synthesis conditions and resulting oxygen contents of the material used in these studies: in the studies by Bi and Zhu and van den Bossche and McIntosh, Sr_2MgMoO_6 was synthesized in air,[87,88] whereas in case of Huang *et al.* it was synthesized under highly reducing conditions.[19,30] With Sr_2MgMoO_6, samples synthesized in air are essentially oxygen stoichiometric, but can be slightly reduced afterwards.[86,III] However, samples synthesized under reducing conditions show

around three to five times as many oxygen vacancies than can be obtained by reducing a sample synthesized in air.[89,II] What is more, oxidation and reduction after the synthesis are reversible and the oxygen content appears to always return to the same value during reduction.[II,III] Thus, the reducibility of this compound seems to be related to the initial synthesis conditions, and the maximum reducibility is set at the synthesis.

This appears to be caused by differences in the *B*-site cation ordering. It has been noted that the degree of cation order in Sr_2MgMoO_6 depends on synthesis conditions; samples synthesized under more reducing conditions have a lower degree of cation order.[86,II,III] This has been explained by the Mg trying to avoid a coordination lower than six. When synthesized under reducing conditions, the compound becomes more disordered in order to create more Mo-O-Mo bonds from where the oxygen can more easily be removed than from the Mg-O-Mo bonds of the fully ordered case.[86] Due to the large charge difference between Mg^{II} and Mo^{VI}, Sr_2MgMoO_6 samples synthesized in air have a high degree of order, with very few Mo-O-Mo bonds, and the samples cannot be reduced much afterwards as the oxygen cannot be removed from the structure. Thus the reducibility of Sr_2MgMoO_6 appears to be limited by the *B*-site cation order. As the electrical and probably also the electrocatalytic properties of this compound depend on the oxygen content,[19] these findings indicate that samples with lower degree cation of order could perform better as SOFC anodes, and may explain the discrepancies found in literature.

3.2 $Sr_2B'MoO_6$ with *B*' = Mn, Fe, Co or Ni

Besides Sr_2MgMoO_6, at least $Sr_2B'MoO_6$ compounds with *B*' = Mn, Fe, Co and Ni have also been tested as SOFC anodes in single cells.[31–34] Compared to Sr_2MgMoO_6, improved electrical conductivities may be possible when *B*' is a transition metal ion, as shown in Table 1, which compares the electrical conductivities reported for $Sr_2B'MoO_6$ with *B*' = Mg, Mn, Co and Ni under reducing conditions. Electrical conductivity values have not been reported for Sr_2FeMoO_6 at high temperatures, but at room temperature it is metallic with electrical conductivity as high as ~1000 S/cm.[I] Also, a transition metal element at the *B*' site could improve the materials catalytic activity compared to Mg.

However, of these compounds Sr_2MnMoO_6 was found to exhibit poorer cell performance than Sr_2MgMoO_6, especially in CH_4, as shown in Table 1, where fuel cell test results reported for these different compounds are compared. Worse sulfur tolerance was also found, as Mn apparently reacts more readily with sulfur than Mg.[19] On the other hand, Sr_2FeMoO_6 has shown rather promising SOFC performance, even with CH_4 as a fuel, as is seen in Table 1. Furthermore, the Sr_2FeMoO_6 cell tests were done using Ag current collectors and no Pt was used, yet the results match those of Sr_2MgMoO_6 with the Pt current collectors.[31] Finally, Sr_2CoMoO_6 has also been found to exhibit very promising performance in both H_2 and CH_4, whereas the results for Sr_2NiMoO_6 have been somewhat poorer, but still worthy of additional study.[32–34]

Table 1. Electrical conductivities at 800 °C under reducing conditions, and fuel-cell test power-densities obtained at H_2 or CH_4.

Compound	Electrical conductivity (S/cm)	Power density with H_2 (W/cm^2)	Power density with CH_4 (W/cm^2)	References
Sr_2MgMoO_6	0.3-9	0.71-0.84	0.34-0.45	[19,30,84],III
Sr_2MnMoO_6	8	0.66	0.12	[19,30]
Sr_2FeMoO_6	-	0.60	0.43	[31]
Sr_2CoMoO_6	2-5	0.74-1.02	0.19-0.45	[32,34]
Sr_2NiMoO_6	0.1-50	0.48-0.6	0.25	[32,33]

For SOFC anode materials, redox stability is of essence. The anode has to be stable in varying atmospheres, because even though the oxygen partial pressure in the anode compartment is very low, it may change several orders of magnitude during the operation. It would also be advantageous if the anode could recover even from brief exposure to air at high temperatures, for example in case of a short break in the fuel feed.

As stated before, Sr_2MgMoO_6 is stable both under oxidizing and reducing conditions. In the present work the redox stability of the other possible SOFC anode materials was examined using TG analysis.[II] $Sr_2B'MoO_6$ compounds with *B*' = Mn or Fe are easily overoxidized due to the stability of the III oxidation state of these elements, and they must be synthesized under reducing conditions. While they are stable in the anode conditions, they may break down if air is introduced to the anode. When heated in air, their oxidation starts already below 400 °C, as shown in Figure 8, resulting in decomposition of the compounds. Due to this low decomposition temperature, lowering the fuel-cell operating temperature would not help. Thus if these compounds were to be used as SOFC anodes, they would have to be carefully protected from air.

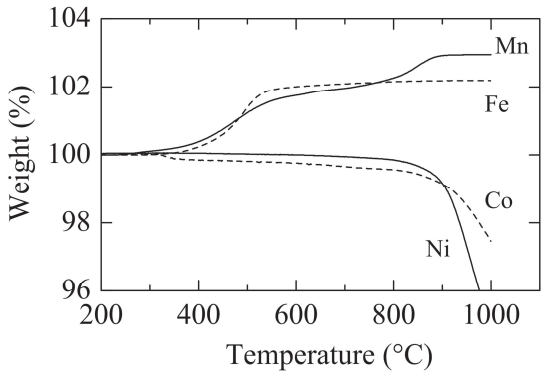

Figure 8. TG measurement results for $Sr_2B'MoO_6$ with *B*' = Mn or Fe in air, and with *B*' = Co or Ni in 5 % H_2/Ar.[II]

On the other hand, $Sr_2B'MoO_6$ compounds with *B*' from the right side of periodic table, Co or Ni, are stable in oxidizing conditions, and can be synthesized in air. However, they are reduced and decomposed easily above 800 °C

under 5 % H_2/Ar, as shown in Figure 8. This different behavior compared to the *B*' = Mn or Fe compounds is caused by the fact that orbital energies of the 3*d* transition metals are lowered with increasing atomic number due to the increase in nuclear charge.[90] The orbital energies in case of *B*' = Co and Ni are low enough to accept electrons and reduce under the reducing atmosphere. This makes their use as SOFC anodes rather difficult: it may be possible to use them at certain situations at low temperatures, below 800 °C, but formation of local hot spots during operation could cause degradation of the anode. During SOFC operation oxygen is transported to the anode from the electrolyte, which might help stabilize the compounds. But if the oxygen flow would stop, the anode could be irreversibly destroyed.

Partial cation substitution at the *B*'-site could provide compounds with good stability and improved anode performance. For example, $Sr_2Mg_{1-x}Co_xMoO_6$ with moderate amounts of Co has been found to be more redox stable than Sr_2CoMoO_6 and to have higher electronic and ionic conductivities than Sr_2MgMoO_6, with samples synthesized in air.[91] The Co-for-Mg substitution was also found to improve fuel cell performance compared to Sr_2MgMoO_6. Similarly, $Sr_2Ni_{0.75}Mg_{0.25}MoO_6$ synthesized in air has been found to exhibit electrical conductivity of 33 S/cm at 800 °C under reducing conditions, at least an order of magnitude higher than Sr_2MgMoO_6, and the Mg improves the material's redox stability compared to pure Sr_2NiMoO_6.[92]

3.3 $Sr_2MgMo_{1-x}B''_xO_6$ with *B*'' = Nb or W

Compared to the Mg-site substitution, the effects of substituting the Mo site of Sr_2MgMoO_6 have been studied much less. In this work the effects of substituting Mo^{VI} by Nb^{V} or W^{VI} were examined.[III] Of these two, the isovalent substitution by W was found to cause relatively small changes to the structure as even the ionic radii[93] of Mo (0.59 Å) and W (0.60 Å) are almost identical. On the other hand, the aliovalent substitution by Nb was found to create a large number of oxygen vacancies in the structure, as shown in Figure 9, due to the lower oxidation state of Nb^{V} compared to Mo^{VI}.

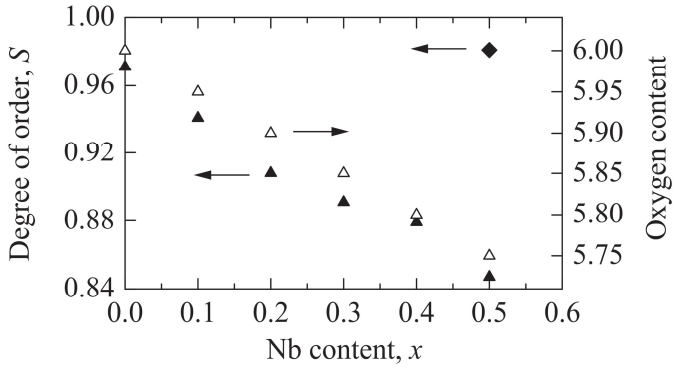

Figure 9. Oxygen content (Δ) and *B*-site cation degree of order (▲) for $Sr_2MgMo_{1-x}Nb_xO_6$ as a function of *x*.[III] Also shown is the *B*-site cation degree of order for $Sr_{1.5}La_{0.5}MgMo_{0.5}Nb_{0.5}O_6$ (♦).

It was discussed earlier how the *B*-site cation order and oxygen content are correlated in Sr_2MgMoO_6. The Nb-for-Mo substitution in Sr_2MgMoO_6 exemplifies this behavior quite clearly. Nb substitution creates oxygen vacancies in the structure, and at the same time the degree of *B*-site cation order is strongly decreased, as shown in Figure 9; with the Nb substitution level in $Sr2MgMo_{1-x}Nb_xO_6$ increasing from $x = 0$ to 0.5 the cation degree of order decreases from $S = 0.97$ to 0.85. This reduction of cation order might be assumed to be caused by the smaller charge and size difference between Mg^{II} (ionic radius 0.72 Å) and Nb^{V} (0.64 Å) compared to Mo^{VI} (0.59 Å). However, preliminary results obtained for a compound $Sr_{1.5}La_{0.5}MgMo_{0.5}Nb_{0.5}O_6$ (Figure 9), which has no oxygen vacancies, show a high degree of *B*-site order of $S = 0.98$, essentially the same as unsubstituted Sr_2MgMoO_6. This is despite the fact that $Sr_{1.5}La_{0.5}MgMo_{0.5}Nb_{0.5}O_6$ has the same *B*-site cation configuration as $Sr_2MgMo_{0.5}Nb_{0.5}O_6$. Thus it is evident that the oxygen vacancies are in fact the main cause for the decrease in cation order in this series of compounds. This is most likely caused by the same reluctance of Mg to settle with lower coordination as in case of pure Sr_2MgMoO_6.

Both the Nb or W substituted Sr_2MgMoO_6 samples were stable under reducing conditions, and reductions and oxidations were reversible, as with Sr_2MgMoO_6.[III] However, the Nb and W substitutions decreased the materials reducibility, as shown in Figure 10. Synthesized in air, all the samples show a very small maximum reducibility. In case of $Sr_2MgMo_{1-x}W_xO_6$ the reducibility decreases slowly with increasing *x*. This is probably due to W^{VI} being more difficult to reduce to V oxidation state than Mo^{VI}, as evidenced by their standard electrode reduction potentials[94,95] (~0.7 V for $Mo^{VI/V}$ and ~0 V for $W^{VI/V}$). In case of $Sr_2MgMo_{1-x}Nb_xO_6$ the decrease in reducibility with increasing *x* is much faster. The redox potential for $Nb^{V/IV}$ (~-0.2 V) is even lower than that for $W^{VI/V}$, but a more probable reason for this suppression of reducibility is the aforementioned fact that Nb substitution creates oxygen vacancies in the structure and there will thus be less oxygen to remove from the structure to begin with.

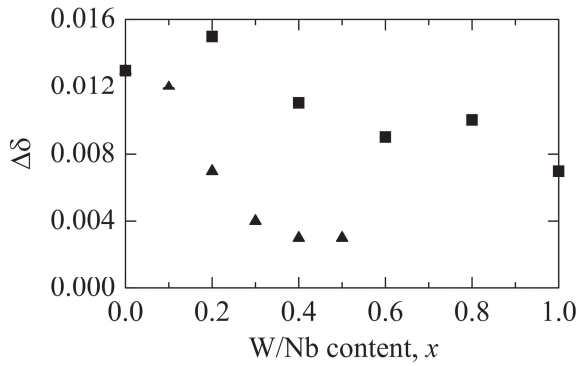

Figure 10. Maximum reducibility of $Sr_2MgMo_{1-x}Nb_xO_6$ (▲) and $Sr_2MgMo_{1-x}W_xO_6$ (■) as a function of x.[III]

When substituting the redox active Mo of Sr_2MgMoO_6 with another cation, it is interesting to consider which of these elements are affected by a reduction. XAS is a useful method for studying this, as it is an element specific method capable of determining changes in oxidation states.

The reducibility of these compounds is small, as discussed above, and x-ray absorption edge energy shifts did not show a clear difference between oxygen stoichiometric and reduced compounds. On the other hand, the transition metal $L_{2,3}$ edge absorption intensities did show a small but consistent effect: for example, in case of a reduced Sr_2MgMoO_6 sample, the Mo $L_{2,3}$ edge absorption feature intensity related to a t_{2g}-derived end state was decreased compared to an oxygen stoichiometric sample, indicating increased electron occupancy of this band, *i.e.* reduction.[III] The XAS measurements indicated that in the $Sr_2MgMo_{1-x}Nb_xO_6$ series Nb was reduced instead of Mo, whereas in the $Sr_2MgMo_{1-x}W_xO_6$ series both Mo and W were reduced simultaneously. The reduction of Nb instead of Mo is somewhat surprising, as standard electrode potentials would predict a contrary behavior. It could be that the oxygen vacancies generated by the Nb substitution are located next to the Mo ions, which might hinder additional removal of oxygen from the vicinity of Mo, and thus prevent Mo from being reduced. Additional NPD or XAS investigations of the *B*-site cation coordinations might be able to shed some light on this subject.

Electrical conductivity is of importance for SOFC anode materials, as stated before. Substitution of Mo in Sr_2MgMoO_6 by Nb or W was found to decrease the material's electrical conductivity, as shown in Figure 11.[III] This behavior is probably related to the decrease in reducibility, which results in less charge carriers during reduction. However, the W-for-Mo substitution reduces the conductivity more than Nb, even though an opposite behavior was seen in the reducibility. As W substitution also does not provide any notable benefits, the $Sr_2MgMo_{1-x}W_xO_6$ compounds appear not to be useful as SOFC anodes. On the other hand, small amounts of Nb substitution in the order of a few percent

might be of use despite the decrease in conductivity, as it provides oxygen vacancies which could improve ionic conductivity.

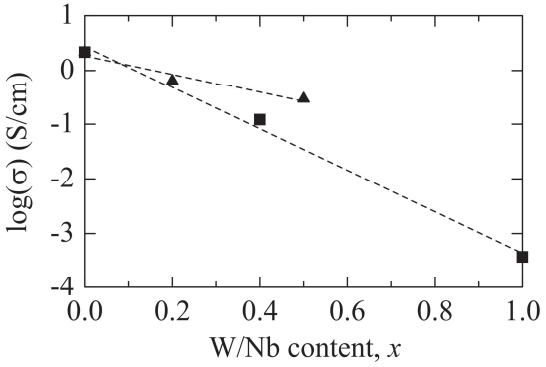

Figure 11. Electrical conductivity of $Sr_2MgMo_{1-x}Nb_xO_6$ (▲) and $Sr_2MgMo_{1-x}W_xO_6$ (■) as a function of *x* at 800 °C under 5 % H_2/Ar.[III]

Escudero *et al.*[96] have in fact studied the properties of $Sr_2MgMo_{0.8}Nb_{0.2}O_6$ from a SOFC anode point of view. The compound showed catalytic activity towards methane partial oxidation when using a CH_4/O_2 gas mixture, and was found to be tolerant to carbon formation. Unfortunately, the compound showed poor electrocatalytic activity. However, the amount of Nb in this composition is rather high and smaller amounts of Nb might be more advantageous.

3.4 $SrMoO_4$ and Composite Anodes

As is evident from the discussion so far, most of the $Sr_2B'MoO_6$-based compounds show relatively low values of electrical conductivity; high enough to be used as SOFC anodes, but much lower than the goal of 100 S/cm. The intrinsic conductivity of these materials may be difficult to increase, but they could be combined with another more conducting material to obtain more highly conductive composite anodes.

$SrMoO_4$ is a common impurity found in the $A_2B'B''O_6$ compounds with Sr and Mo. It is insulating,[97] but can be reduced already below 800 °C to $SrMoO_3$, which has a high metallic conductivity.[98,99] $SrMoO_3$ in itself is not suitable as a SOFC anode, as it shows poor catalytic activity,[100] and as the reduction from $SrMoO_4$ is accompanied by a large change in volume, which could be detrimental to the fuel cell integrity in case of possible reductions and oxidation cycles.[IV] However, $SrMoO_3$ could work as a part of a composite anode, combined with another compound, such as Sr_2MgMoO_6. Figure 12 shows the electrical conductivity of such composites synthesized in air and reduced afterwards.[IV] With an original $SrMoO_4$ content of 30 weight-% or more, the electrical conductivity was notably increased. The conductivity also changed to metallic type, as expected for $SrMoO_3$. Furthermore, the composites showed no

sign of degradation during consecutive reduction and oxidation cycles. $SrMoO_3$ could thus work as a part of a carbon tolerant all-ceramic anode, providing high electrical conductivity with the other anode component working as the electrocatalyst and ionic conductor.

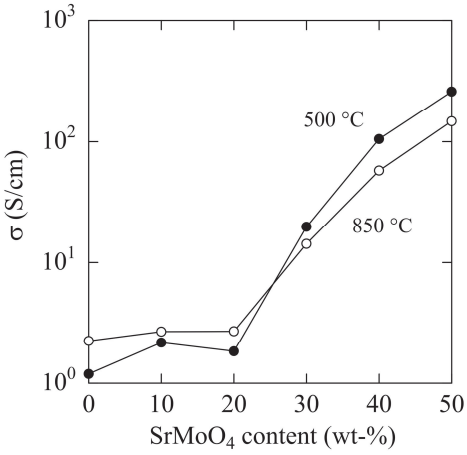

Figure 12. Electrical conductivity of reduced Sr_2MgMoO_6-$SrMoO_4$ composites under 5 % H_2/Ar.[IV]

4. Frustrated and Low-Dimensional Magnetism

Magnetically frustrated compounds have been of great interest in fundamental solid-state physics for decades. Frustration suppresses long-range magnetic order, and compounds with magnetic frustration may offer interesting physical phenomena and ground states, such as spin glass, spin liquid or spin ice.[101–103] Frustrated magnetic behavior has been found in the $A_2B'B''O_6$ perovskites in various forms,[I] making these compounds of interest in this field.

Spin glasses are compounds in which the magnetic frustration is caused by chemical disorder of the magnetic elements.[101] Several disordered $A_2B'B''O_6$ perovskite compounds have been found to exhibit spin-glass-type behavior, with no apparent conventional long-range magnetic order.[9,104,105] This behavior is dependent on the degree of *B*-site cation order, with more ordered samples showing less of a frustrated behavior.[106] However, Sr_2CaReO_6[107] and Sr_2MgReO_6[10] have been reported to show spin-glass-like behavior even with high degree of *B*-site cation order, indicating a different type of magnetic frustration in these compounds.

Geometrical magnetic frustration can happen without disorder.[108] In this case the magnetic ions must form a geometric lattice where the magnetic interactions cannot be properly satisfied. The ideal cubic *B*-site ordered $A_2B'B''O_6$ perovskite forms a tetrahedral system of *B*' (or *B*") cations. This is one of the geometries where antiferromagnetic nearest-neighbor (NN) interactions may become frustrated.[48,109] Next-nearest-neighbor (NNN) interactions may lift this frustration, although cases with small spin values may form exceptions.[110,111] This geometric frustration is exemplified in many ordered $A_2B'B''O_6$ perovskites where no magnetic order is found.[I]

The geometric frustration of the NN interactions may be destroyed by the NNN interactions, but competition between the two different interactions may also be a source of frustration. The different NN and NNN interactions would favor different magnetic orderings, and thus frustration in the spin orientation is expected if the interactions are comparable.[112] The $A_2B'B''O_6$ lattice may be interesting in the study of this phenomenon, as the NN and NNN interactions in these compounds may be similar in strength.[35,I]

Besides magnetic frustration, low-dimensional magnetic systems have also gained much attention in solid-state physics, partly because the parent phases of high-T_c copper-oxide superconductors are two-dimensional antiferromagnets. Furthermore, the superconductivity of these compounds is believed to be connected to their magnetic properties.[113–115] Even without superconductivity, such low-dimensional systems may exhibit intriguing ground state properties, especially if their magnetic interactions are frustrated.[116,117]

Considering both low-dimensional magnetism and magnetic frustration, $A_2CuB''O_6$-type double perovskites are of interest. While relative few in num-

bers, these compounds have been found to show various different magnetic properties depending on their composition.[35–44] However, their magnetic properties have not been thoroughly studied and compared as a group before, so in this work this task was begun.

4.1 $Sr_2CuB''O_6$ with *B*" = Mo, Te, W, Os or Ir

At room temperature, $Sr_2CuB''O_6$ with hexavalent *B*" = Mo, Te, W, Os or Ir are tetragonal ($c/a\sqrt{2} \approx 1.09$-1.11), due to a cooperative Jahn-Teller (JT) distortion of the $Cu^{II}O_{6/2}$ octahedra.[36,43,118–121,V,VI] The four short Cu-O_{ab} bonds lie in the *ab* planes, whereas the two long Cu-O_c bonds are ordered along the *c* axis.

When *B*" is a nonmagnetic ion, *i.e.* Mo^{VI}, Te^{VI} or W^{VI}, the $Sr_2CuB''O_6$ compounds show a quasi-low-dimensional magnetic behavior, with a broad maximum in the magnetic susceptibility,[35,36,V,VI] as shown in Figure 13 for Sr_2CuWO_6 and Sr_2CuMoO_6 as an example. In these compounds Cu is the only magnetically active ion. Because of the cooperative JT distortion, the half-filled Cu d_{x2-y2} orbitals are ordered into the *ab* plane, whereas the orbitals pointing towards the *c* direction (d_{z2}, d_{yz}, and d_{zx}) are filled. This results in relatively strong magnetic interactions between the Cu ions within the *ab* plane, but weaker interactions in the *c* direction. The Cu ions effectively form a square lattice, making the magnetic interactions quasi-two-dimensional.

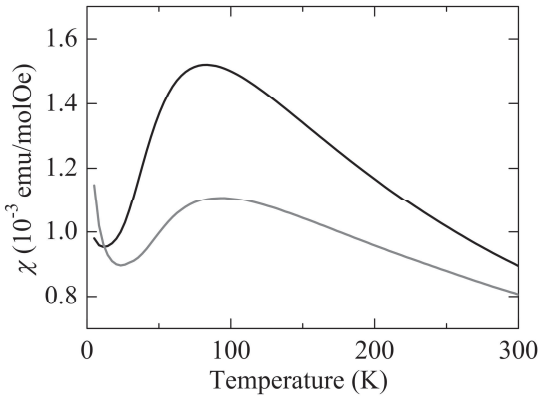

Figure 13. Magnetic susceptibility of Sr_2CuWO_6 (black) and Sr_2CuMoO_6 (gray) as a function of temperature.[V,VI]

While the $Sr_2CuB''O_6$ compounds with d^0 *B*" cations Mo^{VI}, W^{VI} or Te^{VI} show quasi-low-dimensional magnetic behavior, Sr_2CuOsO_6 with a d^2 Os^{VI} has been found to show only a very minor broadening in the magnetic susceptibility.[43] Sr_2CuIrO_6 with a d^3 Ir^{VI}, on the other hand, showed no broadening in susceptibility, but instead a sharp maximum, reminiscent of a typical AFM, as can be seen in Figure 14.[VIII] This progressive change from quasi-low-dimensional behavior to a more typical AFM indicates that the paramagnetic cation at the *B*" site can destroy the magnetic anisotropy of the Cu lattice by introducing

additional magnetic interactions between Cu and the *B*" ion. It is also evident that the strength of these interactions is related to the number of *d* electrons of the *B*" cation. Sr_2CuReO_6 with a d^1 Re^{VI} would be an interesting addition to this group of compounds. However, it has not been synthesized yet, and preliminary synthesis tests during this work resulted in a mixture of phases with Re^{VII} and Cu^{I}, with no perovskite phase forming.

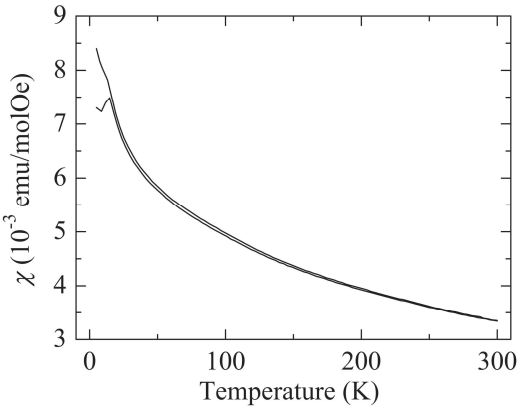

Figure 14. Magnetic susceptibility of Sr_2CuIrO_6 as a function of temperature.[VIII]

The Sr_2Cu*B*"O_6 compounds with *B*" = Os and Ir show a divergence between zero-field-cooled (ZFC) and field-cooled (FC) susceptibilities at low temperatures,[43,VIII] which is not seen in the other Sr_2Cu*B*"O_6 compounds. Such divergence has been found in other A_2*B*'*B*"O_6 perovskites, and is often related to a spin-glass-type behavior.[104,105,122–125] However, Sr_2CuOsO_6 and Sr_2CuIrO_6 show practically complete cation order, which would exclude a typical spin-glass behavior. This would indicate that the divergence in susceptibility is in fact due to frustration between the different magnetic interactions in these compounds. The magnetic exchange interaction constants have been calculated in case of Sr_2CuOsO_6, and the results did indeed indicate frustrated magnetic interactions.[72]

4.2 Long-Range Order in Sr_2CuWO_6 and Sr_2CuMoO_6

It is clear that in this family of A_2Cu*B*"O_6 compounds the magnetic properties can be strongly affected by their composition, making them a useful system for studying the various magnetic interactions. Thus determining their magnetic ground states is of interest in the study of the borderline between the quasi-low-dimensional and three-dimensional magnetic properties.

In this work the possibility of magnetic long-range order in Sr_2CuWO_6 and Sr_2CuMoO_6 was studied.[VI,VII] As stated before, these compounds show low-dimensional behavior in their magnetic susceptibilities. However, μSR measurements were able to show that Sr_2CuWO_6 and Sr_2CuMoO_6 have long-range

magnetic order below T_N of 24(1) and 28(1) K, respectively.[VI] The evolution of the local magnetic fields as a function of temperature in these compounds, shown in Figure 15, also suggests a development of a typical three-dimensional ordered state.

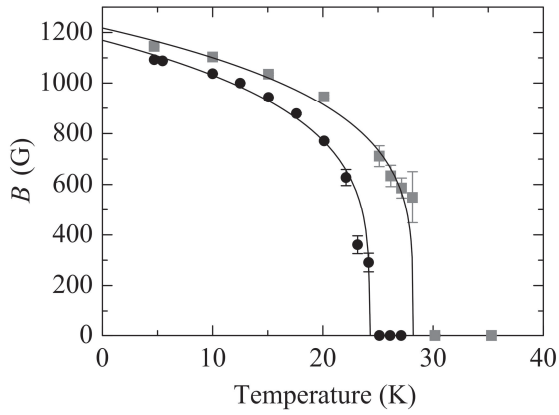

Figure 15. Development of local magnetic fields in Sr_2CuWO_6 (black spheres) and Sr_2CuMoO_6 (gray squares) as a function of temperature.[VI]

In order to verify the long-range order and to determine the actual magnetic ground state, NPD was used to determine the magnetic structure in case of Sr_2CuWO_6.[VII] The magnetic reflections of this sample were found to be very weak and a high-flux instrument was needed in order to detect the reflections. With such an instrument clear magnetic reflections could be seen at temperatures below T_N, as shown in Figure 16. Rietveld refinement of the magnetic reflections showed the magnetic order to be of type-II AFM order of the double perovskite lattice, with a propagation vector k = (0,½,½) with respect to the tetragonal unit cell. This magnetic order is indicative of strong AFM NNN interactions between the Cu ions.[106,126,I] The NPD results also showed that the Cu spins are oriented along the a axis of the structure, as can be seen in Figure 16. NPD experiment was not attempted in case of the HP synthesized Sr_2CuMoO_6, as the sample amount was small and the magnetic reflections were found to be difficult to detect already in case of Sr_2CuWO_6.

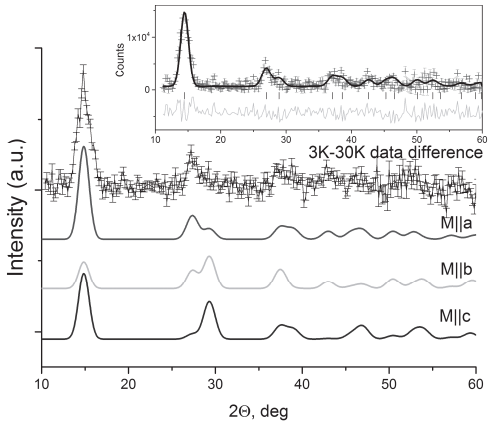

Figure 16. Difference curve of NPD data measured at 3 and 30 K and simulated patterns with Cu magnetic moment along *a*, *b* or *c* axes. Inset shows a Rietveld refinement result with moments along the *a* axis.[VII]

4.3 Exchange Interactions in Sr_2CuWO_6 and Sr_2CuMoO_6

In order to shed more light on the case of magnetic ordering in Sr_2CuWO_6 and Sr_2CuMoO_6, the most relevant magnetic exchange constants of these compounds were calculated using DFT.[VI] In the tetragonal case the magnetic interactions within the *ab* plane and along the *c* directions differ. Figure 17 shows these interactions between the Cu ions: J_1 and J_2 are the NN and NNN interactions in the *ab* plane, and J_3 and J_4 are the NN and NNN interactions along the *c* direction, respectively.

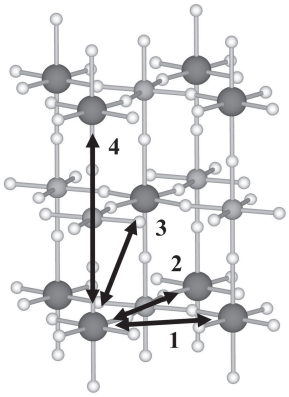

Figure 17. Schematic of the magnetic exchange constants J_1-J_4 between Cu ions (large dark-gray spheres) in $Sr_2Cu(W,Mo)O_6$. Small gray spheres represent W/Mo and small white spheres are O.

The calculated exchange constants were found to be qualitatively similar for both Sr_2CuWO_6 and Sr_2CuMoO_6. The results indicated that the quasi-low-

dimensional properties of these compounds are caused by relatively strong NNN interactions J_2 within the ab-plane. Furthermore, these interactions appear to be slightly frustrated by the NN interactions J_1. On the other hand, the low-temperature long-range order in these compounds is caused by the NNN interaction J_4 along the c axis. The strong NNN interactions would favor a type-II magnetic order, as was found in case of Sr_2CuWO_6. Based on these results, it is expected that the magnetic ground state of Sr_2CuMoO_6 is also of type-II AFM.

4.4 $Ba_2CuW_{1-x}U_xO_6$

The discussion this far has only considered $A_2CuB"O_6$ compounds with A = Sr. However, compounds with A = Ba have been found to exhibit similarly interesting magnetic behavior.[35–42,44] For example, Ba_2CuWO_6 shows a quasi-low-dimensional behavior comparable to Sr_2CuWO_6, but another very similar compound Ba_2CuUO_6 with nonmagnetic U^{VI} has been reported to be either a quasi-two-dimensional compound[37,38] or a typical antiferromagnet.[39,40] Preliminary susceptibility data measured for a series of $Ba_2CuW_{1-x}U_xO_6$ compounds (Figure 18) show a transition from low-dimensional behavior with strongly suppressed susceptibility to a more typical AFM behavior when x is increased. Up to x = 0.8, there is no clear indication of a transition to a long-range ordered state in the susceptibility data of this series. Ba_2CuUO_6 (x = 1) on the other hand has a sharp susceptibility maximum at T_N = 10 K, as has also been found in literature.[39,40]

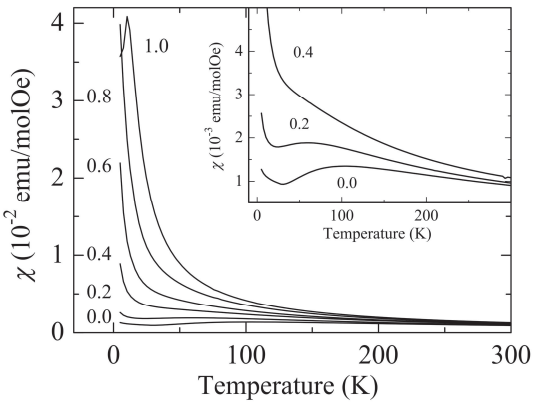

Figure 18. Magnetic susceptibilities of a series of $Ba_2CuW_{1-x}U_xO_6$ compounds as a function of temperature. Inset shows compounds with x = 0.0-0.4 in close-up.

While magnetic long-range order is not obvious in the magnetic susceptibility of most of these compounds, Todate *et al.*[42] showed Ba_2CuWO_6 to have a three-dimensional ordered state below T_N = 28 K. NPD study also showed the long-range ordered state to be of type-II AFM, with a magnetic propagation vector of k = (0,½,½) with respect to the tetragonal unit cell. As stated before,

this type of order is caused by relatively strong AFM NNN interactions between the Cu ions. Ba_2CuUO_6 on the other hand has been found to have a magnetic order with a propagation vector of k = (½,½,0),[37,40] indicating relatively strong AFM NN interactions with ferromagnetic NNN interactions. The Weiss temperatures of these compounds also change from ~-200 K to ~10 K when moving from Ba_2CuWO_6 to Ba_2CuUO_6, exhibiting an increase in the strength of ferromagnetic interactions.

The progress from low-dimensional to a more typical AFM behavior in this series is somewhat similar to what was seen in case of the $Sr_2Cu\mathit{B}"O_6$ compounds. However, a crucial difference in the $Ba_2CuW_{1-x}U_xO_6$ series is that U^{VI} is also diamagnetic, with no *d* or *f* electrons, similar to W^{VI}. The change in magnetic behavior is thus not related to additional magnetic interactions, but to more subtle effects, such as changes in bond-lengths and distances or in energetic orbital overlaps.

5. Conclusions

Materials with improved or completely new properties are important for the future technological development. Discovering such novel materials requires an understanding of the basic chemical and physical principles governing their properties. The aim of the present work was to gain an understanding of one group of materials, the $A_2B'B''O_6$ perovskites. These perovskites form a relatively simple system to study, but with greatly varying structural, electronic and magnetic properties, which makes them of interest from a fundamental solid-state chemistry and physics point of view, but also due to their possible applications.

In a more application oriented side of this work, several $A_2B'MoO_6$-type double-perovskite compounds intended as SOFC anode materials were studied. The reducibility of the most studied of these compounds, Sr_2MgMoO_6, has been found to be affected by its *B*-site cation ordering. This effect was especially notable in case of the aliovalent Nb-for-Mo substitution of Sr_2MgMoO_6, where a strong correlation between oxygen vacancies and cation order was noted. This behavior is intriguing considering order-disorder phenomena in solid compounds in general, and would require additional examination. From the SOFC anode point of view, properties of Sr_2MgMoO_6 could perhaps be improved by lowering the degree of cation order using different synthesis conditions.

Replacing Mg in Sr_2MgMoO_6 by transition metals elements was also examined in this thesis. The $Sr_2B'MoO_6$ compounds with a transition metal at the *B*' site were found not to be redox stable by themselves, but different amounts of these elements substituted at the Mg site of Sr_2MgMoO_6 could prove advantageous, providing samples with improved performance yet sufficient redox stability. Similarly, small scale substitution of the electrocatalytically active Mo might be of interest, as in case of the Nb-for-Mo substitution, which can provide oxygen vacancies in the structure. However, as was found in this work, too much of Nb can severely lower the material's reducibility and electrical conductivity. In these perovskites a wide range of partial cation substitution combinations are possible, and the best composition is not yet known, leaving room for future improvement of these materials. Finally, if a single compound with optimal properties is not found, composite anodes combining the best properties of two different compounds could be considered.

The $A_2B'B''O_6$ perovskites also show a great range of different magnetic properties, ranging from the more typical ferro- ferri- or antiferromagnetic orderings to somewhat more uncommon cases with frustrated or low-dimensional behavior. Such materials may not be of immediate use in applications, but they are of great interest in basic research, and can help understand the behavior of other systems such as the high-T_c superconductors. The $A_2CuB''O_6$-type perovskites form a small but intriguing group of compounds

that show varying magnetic properties depending on their composition. The change from quasi-low-dimensional to a more typical AFM behavior is especially interesting. These compounds are still relatively poorly studied as a whole, and a more concentrated study of their properties could prove fruitful.

Two new compounds of this family, Sr_2CuMoO_6 and Sr_2CuIrO_6, were synthesized in the course of this work, and it would be interesting to synthesize and characterize more of these perovskites. For example, the *A* = Ba versions of these two compounds are not known. On the other hand, while Ba_2CuUO_6 is known, synthesis of Sr_2CuUO_6 has been unsuccessful.[39,127] Similarly, Ca_2Cu*B*"O_6 perovskites have not been synthesized, and it has been postulated that the increased structural distortion caused by the small *A* site cation Ca is incompatible with the JT distortion in the structure.[128] However, using different synthesis condition such as high pressure, some of these compounds could perhaps be stabilized.

References

1. A. S. Bhalla, R. Guo, and R. Roy, *Mater. Res. Innov.* **4** (2000) 3.

2. R. H. Mitchell, *Perovskites: Modern and Ancient* (2000) Almaz Press Inc., Thunder Bay.

3. J. B. Goodenough, *Reports Prog. Phys.* **67** (2004) 1915.

4. W. E. Pickett and D. J. Singh, *Phys. Rev. B* **53** (1996) 1146.

5. K.-I. Kobayashi, T. Kimura, H. Sawada, K. Terakura, and Y. Tokura, *Nature* **395** (1998) 677.

6. R. J. Cava, B. Batlogg, J. J. Krajewski, R. Farrow, L. W. Rupp, A. E. White, K. Short, W. F. Peck, and T. Kometani, *Nature* **332** (1988) 814.

7. J. B. Goodenough and J. M. Longo, in *Landolt-Börnstein. Numerical Data and Functional Relationships in Science and Technology, New Series, Group III: Crystal and Solid State Physics. Vol. 4: Magnetic and Other Properties of Oxides and Related Compounds, Part a* (1970) Springer, Berlin, p. 126.

8. J. B. Goodenough, *Magnetism and the Chemical Bond* (1963) Interscience Publishers, New York.

9. P. D. Battle, T. C. Gibb, C. W. Jones, and F. Studer, *J. Solid State Chem.* **78** (1989) 281.

10. C. R. Wiebe, J. E. Greedan, P. P. Kyriakou, G. M. Luke, J. S. Gardner, A. Fukaya, I. M. Gat-Malureanu, P. L. Russo, A. T. Savici, and Y. J. Uemura, *Phys. Rev. B* **68** (2003) 134410.

11. M. Li, M. J. Pietrowski, R. A. De Souza, H. Zhang, I. M. Reaney, S. N. Cook, J. A. Kilner, and D. C. Sinclair, *Nat. Mater.* **13** (2014) 31.

12. H. Hayashi, H. Inaba, M. Matsuyama, N. G. Lan, M. Dokiya, and H. Tagawa, *Solid State Ionics* **122** (1999) 1.

13. H. Tanaka and M. Misono, *Curr. Opin. Solid State Mater. Sci.* **5** (2001) 381.

14. S.-W. Cheong and M. Mostovoy, *Nat. Mater.* **6** (2007) 13.

15. D. I. Khomskii, *J. Magn. Magn. Mater.* **306** (2006) 1.

16. D. E. Kotecki, *Integr. Ferroelectr.* **16** (1997) 1.

17. Y. Moritomo, A. Asamitsu, H. Kuwahara, and Y. Tokura, *Nature* **380** (1996) 141.

18. V. V Kharton, F. M. B. Marques, and A. Atkinson, *Solid State Ionics* **174** (2004) 135.

19. Y.-H. Huang, R. I. Dass, Z.-L. Xing, and J. B. Goodenough, *Science* **312** (2006) 254.

20. H. W. Eng, P. W. Barnes, B. M. Auer, and P. M. Woodward, *J. Solid State Chem.* **175** (2003) 94.

21. M. A. Green, A. Ho-Baillie, and H. J. Snaith, *Nat. Photonics* **8** (2014) 506.

22. P. M. Woodward, *Acta Crystallogr. Sect. B Struct. Sci.* **53** (1997) 32.

23. G. King and P. M. Woodward, *J. Mater. Chem.* **20** (2010) 5785.

24. P. K. Davies, H. Wu, A. Y. Borisevich, I. E. Molodetsky, and L. Farber, *Annu. Rev. Mater. Res.* **38** (2008) 369.

25. M. T. Anderson, K. B. Greenwood, G. A. Taylor, and K. R. Poeppelmeier, *Prog. Solid State Chem.* **22** (1993) 197.

26. E. J. Williams, *Proc. R. Soc. London. Ser. A - Math. Phys. Sci.* **152** (1935) 231.

27. P. M. Woodward, R. D. Hoffmann, and A. Sleight, *J. Mater. Res.* **9** (1994) 2118.

28. D. Serrate, J. M. De Teresa, and M. R. Ibarra, *J. Phys. Condens. Matter* **19** (2007) 023201.

29. M. Karppinen and H. Yamauchi, in *Frontiers in Magnetic Materials*, edited by A. V Narlikar (2005) Springer, Berlin, pp. 153–184.

30. Y.-H. Huang, R. I. Dass, J. C. Denyszyn, and J. B. Goodenough, *J. Electrochem. Soc.* **153** (2006) A1266.

31. Z. Wang, Y. Tian, and Y. Li, *J. Power Sources* **196** (2011) 6104.

32. Y.-H. Huang, G. Liang, M. Croft, M. Lehtimäki, M. Karppinen, and J. B. Goodenough, *Chem. Mater.* **21** (2009) 2319.

33. T. Wei, Y. Ji, X. Meng, and Y. Zhang, *Electrochem. Commun.* **10** (2008) 1369.

34. P. Zhang, Y.-H. Huang, J.-G. Cheng, Z.-Q. Mao, and J. B. Goodenough, *J. Power Sources* **196** (2011) 1738.

35. G. Blasse, *Philips Res. Reports* **20** (1965) 327.

36. D. Iwanaga, Y. Inaguma, and M. Itoh, *J. Solid State Chem.* **147** (1999) 291.

37. A. Murasik, P. Fischer, and A. Zygmunt, *J. Magn. Magn. Mater.* **137** (1994) 139.

38. A. Murasik, P. Fischer, and A. Zygmunt, *J. Magn. Magn. Mater.* **140-144** (1995) 1717.

39. M. D. Marcos and J. P. Attfield, *J. Mater. Chem.* **4** (1994) 475.

40. P. Leporcher, G. André, T. Roisnel, T. Le Bihan, and H. Noël, *J. Alloys Compd.* **213-214** (1994) 506.

41. Y. Todate, *J. Phys. Soc. Jpn.* **70** (2001) 337.

42. Y. Todate, W. Higemoto, K. Nishiyama, and K. Hirota, *J. Phys. Chem. Solids* **68** (2007) 2107.

43. M. W. Lufaso, W. R. Gemmill, S. J. Mugavero, S.-J. Kim, Y. Lee, T. Vogt, and H.-C. zur Loye, *J. Solid State Chem.* **181** (2008) 623.

44. H. L. Feng, M. Arai, Y. Matsushita, Y. Tsujimoto, Y. Yuan, C. I. Sathish, J. He, M. Tanaka, and K. Yamaura, *J. Solid State Chem.* **217** (2014) 9.

45. J. B. Goodenough, J. A. Kafalas, and J. M. Longo, in *Preparative Methods in Solid State Chemistry*, edited by P. Hagenmuller (1972) Academic Press, Inc., New York, pp. 1–69.

46. D.-Y. Jung and G. Demazeau, *J. Solid State Chem.* **115** (1995) 447.

47. J.-H. Choy, D.-K. Kim, S.-H. Hwang, G. Demazeau, and D.-Y. Jung, *J. Am. Chem. Soc.* **117** (1995) 8557.

48. P. Kayser, M. J. Martínez-Lope, J. A. Alonso, M. Retuerto, M. Croft, A. Ignatov, and M. T. Fernández-Díaz, *Inorg. Chem.* **52** (2013) 11013.

49. G. Demazeau, D.-Y. Jung, J.-P. Sanchez, E. Colineau, A. Blaise, and L. Fournes, *Solid State Commun.* **85** (1993) 479.

50. J.-H. Choy, D.-K. Kim, G. Demazeau, and D.-Y. Jung, *J. Phys. Chem.* **98** (1994) 6258.

51. D.-Y. D.-Y. Jung, P. Gravereau, and G. Demazeau, *Eur. J. Solid State Inorg. Chem.* **30** (1993) 1025.

52. H. Yamauchi and M. Karppinen, *Supercond. Sci. Technol.* **13** (2000) R33.

53. D. C. Köningsberger and R. Prins, editors, *X-Ray Absorption: Principles, Applications, Techniques of EXAFS, SEXAFS and XANES* (1988) John Wiley & Sons, New York.

54. M. Gautier-Soyer, *J. Eur. Ceram. Soc.* **18** (1998) 2253.

55. G. Popov, M. Greenblatt, and M. Croft, *Phys. Rev. B* **67** (2003) 24406.

56. J.-H. Choy, J.-Y. Kim, S.-H. Hwang, S.-J. Kim, and G. Demazeau, *Int. J. Inorg. Mater.* **2** (2000) 61.

57. F. M. F. de Groot, M. Grioni, J. C. Fuggle, J. Ghijsen, G. A. Sawatzky, and H. Petersen, *Phys. Rev. B* **40** (1989) 5715.

58. F. M. F. de Groot, J. Faber, J. J. M. Michiels, M. T. Czyzyk, M. Abbate, and J. C. Fuggle, *Phys. Rev. B* **48** (1993) 2074.

59. A. Modin, Y. Yun, M.-T. Suzuki, J. Vegelius, L. Werme, J. Nordgren, P. M. Oppeneer, and S. M. Butorin, *Phys. Rev. B* **83** (2011) 75113.

60. M. Grioni, J. F. van Acker, M. T. Czyzyk, and J. C. Fuggle, *Phys. Rev. B* **45** (1992) 3309.

61. P. Dalmas de Reotier and A. Yaouanc, *J. Phys. Condens. Matter* **9** (1997) 9113.

62. S. J. Blundell, *Contemp. Phys.* **40** (1999) 175.

63. P. Bakule and E. Morenzoni, *Contemp. Phys.* **45** (2004) 203.

64. T. Chatterji, editor, *Neutron Scattering from Magnetic Materials* (2006) Elsevier B. V., Amsterdam.

65. D. S. Scholl and J. A. Steckel, *Density Functional Theory: A Practical Introduction* (2009) John Wiley & Sons, Hoboken.

66. P. Hohenberg and W. Kohn, *Phys. Rev.* **136** (1964) B864.

67. W. Kohn and L. J. Sham, *Phys. Rev.* **140** (1965) A1133.

68. B. Himmetoglu, A. Floris, S. de Gironcoli, and M. Cococcioni, *Int. J. Quantum Chem.* **114** (2014) 14.

69. M.-H. Whangbo, H.-J. Koo, and D. Dai, *J. Solid State Chem.* **176** (2003) 417.

70. D. Dai, H.-J. Koo, and M.-H. Whangbo, *J. Solid State Chem.* **175** (2003) 341.

71. Y. Fujioka, J. Frantti, and R. M. Nieminen, *J. Phys. Chem. B* **112** (2008) 6742.

72. C. Tian, A. C. Wibowo, H.-C. zur Loye, and M.-H. Whangbo, *Inorg. Chem.* **50** (2011) 4142.

73. S. C. Singhall and K. Kendall, editors, *High-Temperature Solid Oxide Fuel Cells: Fundamentals, Design and Applications* (2003) Elsevier B. V., Amsterdam.

74. S. McIntosh and R. J. Gorte, *Chem. Rev.* **104** (2004) 4845.

75. W. Z. Zhu and S. C. Deevi, *Mater. Sci. Eng. A* **362** (2003) 228.

76. E. Ivers-Tiffée, A. Weber, and D. Herbstritt, *J. Eur. Ceram. Soc.* **21** (2001) 1805.

77. R. M. Ormerod, *Chem. Soc. Rev.* **32** (2003) 17.

78. S. P. Jiang and S. H. Chan, *J. Mater. Sci.* **39** (2004) 4405.

79. A. Atkinson, S. Barnett, R. J. Gorte, J. T. S. Irvine, A. J. McEvoy, M. Mogensen, S. C. Singhal, and J. Vohs, *Nat. Mater.* **3** (2004) 17.

80. P. M. Woodward, J. Goldberger, M. W. Stoltzfus, H. W. Eng, R. A. Ricciardo, P. N. Santhosh, P. Karen, and A. R. Moodenbaugh, *J. Am. Ceram. Soc.* **91** (2008) 1796.

81. S. Tao and J. T. S. Irvine, *J. Mater. Chem.* **12** (2002) 2356.

82. S. Tao, J. Canales-Vázquez, and J. T. S. Irvine, *Chem. Mater.* **16** (2004) 2309.

83. T. Xia, Q. Li, J. Meng, and X. Cao, *Mater. Chem. Phys.* **111** (2008) 335.

84. D. Marrero-López, J. Peña-Martínez, J. C. Ruiz-Morales, D. Pérez-Coll, M. A. G. Aranda, and P. Núñez, *Mater. Res. Bull.* **43** (2008) 2441.

85. D. Marrero-López, J. Peña-Martínez, J. C. Ruiz-Morales, M. C. Martín-Sedeño, and P. Núñez, *J. Solid State Chem.* **182** (2009) 1027.

86. C. Bernuy-Lopez, M. Allix, C. A. Bridges, J. B. Claridge, and M. J. Rosseinsky, *Chem. Mater.* **19** (2007) 1035.

87. Z. H. Bi and J. H. Zhu, *J. Electrochem. Soc.* **158** (2011) B605.

88. M. van den Bossche and S. McIntosh, *J. Mater. Chem.* **21** (2011) 7443.

89. Y. Matsuda, M. Karppinen, Y. Yamazaki, and H. Yamauchi, *J. Solid State Chem.* **182** (2009) 1713.

90. Y. S. Lee, J. S. Lee, T. W. Noh, D. Y. Byun, K. S. Yoo, K. Yamaura, and E. Takayama-Muromachi, *Phys. Rev. B* **67** (2003) 113101.

91. Z. Xie, H. Zhao, Z. Du, T. Chen, N. Chen, X. Liu, and S. J. Skinner, *J. Phys. Chem. C* **116** (2012) 9734.

92. E. A. Filonova, A. S. Dmitriev, P. S. Pikalov, D. A. Medvedev, and E. Y. Pikalova, *Solid State Ionics* **262** (2014) 365.

93. R. D. Shannon, *Acta Crystallogr., Sect. A: Found. Crystallogr.* **32** (1976) 751.

94. G. Milazzo and S. Caroli, editors, *Tables of Standard Electrode Potentials* (1978) John Wiley & Sons, New York.

95. S. G. Bratsch, *J. Phys. Chem. Ref. Data* **18** (1989) 1.

96. M. J. Escudero, I. Gómez de Parada, A. Fuerte, and L. Daza, *J. Power Sources* **243** (2013) 654.

97. J. C. Sczancoski, L. S. Cavalcante, M. R. Joya, J. A. Varela, P. S. Pizani, and E. Longo, *Chem. Eng. J.* **140** (2008) 632.

98. I. Nagai, N. Shirakawa, S. Ikeda, R. Iwasaki, H. Nishimura, and M. Kosaka, *Appl. Phys. Lett.* **87** (2005).

99. T. Maekawa, K. Kurosaki, H. Muta, M. Uno, and S. Yamanaka, *J. Alloys Compd.* **390** (2005) 314.

100. B. H. Smith and M. D. Gross, *Electrochem. Solid-State Lett.* **14** (2011) B1.

101. K. Binder and A. P. Young, *Rev. Mod. Phys.* **58** (1986) 801.

102. L. Balents, *Nature* **464** (2010) 199.

103. H. T. Diep, editor, *Frustrated Spin Systems* (2004) World Scientific, Singapore.

104. C. Schinzer, *J. Alloys Compd.* **288** (1999) 65.

105. P. D. Battle, T. C. Gibb, A. J. Herod, and J. P. Hodges, *J. Mater. Chem.* **5** (1995) 75.

106. S. J. Makowski, J. A. Rodgers, P. F. Henry, J. P. Attfield, and J.-W. G. Bos, *Chem. Mater.* **21** (2008) 264.

107. C. R. Wiebe, J. E. Greedan, G. M. Luke, and J. S. Gardner, *Phys. Rev. B* **65** (2002) 144413.

108. A. P. Ramirez, *Annu. Rev. Mater. Sci.* **24** (1994) 453.

109. E. Granado, J. W. Lynn, R. F. Jardim, and M. S. Torikachvili, *Phys. Rev. Lett.* **110** (2013) 17202.

110. M. A. de Vries, A. C. Mclaughlin, and J.-W. G. Bos, *Phys. Rev. Lett.* **104** (2010) 177202.

111. A. C. Mclaughlin, M. A. de Vries, and J.-W. G. Bos, *Phys. Rev. B* **82** (2010) 94424.

112. A. A. Aczel, D. E. Bugaris, L. Li, J.-Q. Yan, C. de la Cruz, H.-C. zur Loye, and S. E. Nagler, *Phys. Rev. B* **87** (2013) 14435.

113. R. J. Cava, *J. Am. Ceram. Soc.* **83** (2000) 5.

114. E. W. Hudson, K. M. Lang, V. Madhavan, S. H. Pan, H. Eisaki, S. Uchida, and J. C. Davis, *Nature* **411** (2001) 920.

115. J. C. S. Davis and D.-H. Lee, *Proc. Natl. Acad. Sci.* **110** (2013) 17623.

116. N. Shannon, B. Schmidt, K. Penc, and P. Thalmeier, *Eur. Phys. J. B - Condens. Matter Complex Syst.* **38** (2004) 599.

117. I. Bose, *Curr. Sci.* **88** (2005).

118. D. Reinen and H. Weitzel, *Z. Anorg. Allg. Chem.* **424** (1976) 31.

119. Bokhimi, *Powder Diffr.* **7** (1992) 228.

120. M. Gateshki and J. M. Igartua, *J. Phys. Condens. Matter* **15** (2003) 6749.

121. M. Gateshki, J. M. M. Igartua, and E. Hernández-Bocanegra, *J. Phys. Condens. Matter* **15** (2003) 6199.

122. M. Gateshki, L. Suescun, S. Kolesnik, J. Mais, K. Swierczek, S. Short, and B. Dabrowski, *J. Solid State Chem.* **181** (2008) 1833.

123. R. Rodríguez, A. Fernández, A. Isalgué, J. Rodríguez, A. Labrata, J. Tejada, and X. Obradors, *J. Phys. C Solid State Phys.* **18** (1985) L401.

124. N. Kashima, K. Inoue, T. Wada, and Y. Yamaguchi, *Appl. Phys. A* **74** (2002) s805.

125. P. D. Battle, T. C. Gibb, A. J. Herod, S.-H. Kim, and P. H. Munns, *J. Mater. Chem.* **5** (1995) 865.

126. P. D. Battle and C. W. Jones, *J. Solid State Chem.* **78** (1989) 108.

127. A. V. Knyazev, N. G. Chernorukov, Z. S. Dashkina, E. N. Bulanov, and I. V. Ladenkov, *Russ. J. Inorg. Chem.* **56** (2011) 888.

128. M. W. Lufaso and P. M. Woodward, *Acta Crystallogr. Sect. B Struct. Sci.* **60** (2004) 10.

Aalto-DD 173/2014

ISBN 978-952-60-5936-5 (printed)
ISBN 978-952-60-5937-2 (pdf)
ISSN-L 1799-4934
ISSN 1799-4934 (printed)
ISSN 1799-4942 (pdf)

Aalto University
School of Chemical Technology
Department of Chemistry
www.aalto.fi

BUSINESS +
ECONOMY

ART +
DESIGN +
ARCHITECTURE

SCIENCE +
TECHNOLOGY

CROSSOVER

**DOCTORAL
DISSERTATIONS**